Naval Research Laboratory

Washington, DC 20375-5000

NRL Memorandum Report 6741

Fiber Optic Feed

DENZIL STILWELL, MARK PARENT AND LEW GOLDBERG*

Radar Analysis Branch
Radar Division

**Optical Techniques Branch*
Optical Sciences Division

November 6, 1990

REPORT DOCUMENTATION PAGE

Form Approved
OMB No. 0704-0188

1. AGENCY USE ONLY (Leave blank)	2. REPORT DATE	3. REPORT TYPE AND DATES COVERED
	1990 November 6	Memorandum 1985-1990

4. TITLE AND SUBTITLE

Fiber Optic Feed

5. FUNDING NUMBERS

53-0611-A0

6. AUTHOR(S)

P. D. Stilwell, M. G. Parent, L. Goldberg *

7. PERFORMING ORGANIZATION NAME(S) AND ADDRESS(ES)

Naval Research Laboratory
Washington, DC 20375-5000

8. PERFORMING ORGANIZATION REPORT NUMBER

NRL Memorandum
Report 6741

9. SPONSORING/MONITORING AGENCY NAME(S) AND ADDRESS(ES)

ONT, Department of the Navy
800 N. Quincy Street
Mr. Jim Hall (ONT-214)
Arlington, VA 22203

10. SPONSORING/MONITORING AGENCY REPORT NUMBER

11. SUPPLEMENTARY NOTES

*Optical Techniques Branch, Optical Sciences Division

12a. DISTRIBUTION/AVAILABILITY STATEMENT

Approved for public release; distribution unlimited.

12b. DISTRIBUTION CODE

13. ABSTRACT *(Maximum 200 words)*

This report details a Fiber Optic Feeding (FOF) concept for beamforming in phased arrays. Experimental data is presented which validates the basic underlying assumptions. Elaborations on this basic concept are presented which illustrate the power of this new approach to beamforming. All radar and communications functions have a realization in the architecture, including monopulse, multiple beams (on same or different frequencies), beamspace adaptivity (open or closed loop), and wideband beam and null forming. It presumes an active antenna aperture but uses TR modules containing no phase shifters. Identical TR modules are used at each of the antenna elements and which require a minimum of digitally controlled components. The architecture is appropriate for arrays on any platform and accommodates sparse and/or conformal designs without the necessity of introducing significant microwave modifications. The approach can use existing state-of-the-art components to affordably implement high performance arrays. Of particular importance is the capability of forming time delay beams from an array without the use of phase shifters.

14. SUBJECT TERMS		15. NUMBER OF PAGES
Array antennas, Time delay beamforiing	Fiber optics	48
		16. PRICE CODE

17. SECURITY CLASSIFICATION OF REPORT	18. SECURITY CLASSIFICATION OF THIS PAGE	19. SECURITY CLASSIFICATION OF ABSTRACT	20. LIMITATION OF ABSTRACT
UNCLASSIFIED	UNCLASSIFIED	UNCLASSIFIED	SAR

CONTENTS

I INTRODUCTION 1

II FOF SYSTEMS CONCEPT 2

II-1 Optical Corporate Feed 2
II-2 Optical Beamsteering 4
II-3 K-Space/Beamspace Diagrams 6

III EXPERIMENTAL RESULTS 7

IV MULTIPLE BEAM FORMATION 10

IV-1 Dependent Beams (Pattern Synthesis) 10
IV-2 Independent Multiple Beams (Anti-Jam) 11
IV-3 Time Dependent Beams (Chirp) 13
IV-4 True Time Delay Beams (Wideband) 14

V CONCLUSIONS AND FUTURE EFFORTS 16

VI APPENDICES 18

VI-1 Optical Detection and Mixing 18
VI-2 Faraday Cell 18
VI-3 Bragg Cell 18
VI-4 Corporate Fed Array 19

FIBER OPTIC FEED

INTRODUCTION

This report concerns R&D performed under the Surface Surveillance Block Program at NRL directed to the use of optical and fiber optical technologies in the implementation of phased array systems, particularly radars. Arrays consist of a set of discrete radiating elements wherein the signal driving each element, whether from the transmitter or from a reflection from a target in the far field, is a time shifted version of the signal at any other element. Time delay arrays are difficult to implement directly (save for a mechanically scanned, space fed array) so present day emphasis has been on phased arrays, in which the signals are delayed at most by one cycle at the radiating frequency. This is normally accomplished with phase shifters, of either a ferrite or a diode type, located at each antenna element.

The Fiber Optic Feed (FOF) program represents an alternative method of obtaining a discrete set of signals with the proper phase shifts for electronic beamforming. This method impresses the microwave frequency on an optical carrier in one leg of an interferometer. In the other it generates a scanned optical beam. The superimposed optical fields are sampled with a fiber array. The optical carrier from each fiber signal is stripped off by heterodyne detection after it has been routed to the proper antenna element. The resulting set of signals exhibits the proper phase shifts for directing beams anywhere in the antenna half space. The technique exploits the similarity between optical beam scanning at a wavelength scale of the order of a micron, and microwave beam formation at a scale of 1-100 cm. This process configures an optically scaled version of the array antenna. Very small time delays occurring from a slight divergence angle between the reference and scanned beam create the requisite phase shifts to steer microwave beams. Quite surprisingly, a simple elaboration of the system makes the phase shift from element to element dependent on microwave frequency in such a manner that time delay beamforming can be realized. Consequently, this architecture is capable of wide instantaneous bandwidth for electronically steered beams at large angles from broadside with no broadening due to bandwidth.

The successful development of the FOF approach would have a significant impact on the utility of array antennas in Naval systems. It would allow for a significant reduction in weight and size while increasing flexibility due to the replacement of microwave transmission lines with fiber optics. It would simplify requisite transmit-receive (TR) modules driving the antenna elements by an elimination of the phase shifter section and accompanying digital control circuitry. It would decrease vulnerability to RFI and EMP while being only marginally more susceptible to ionizing radiation. These properties can be

Manuscript approved August 30, 1990.

translated into reduced system cost and complexity, allowing a wider range of Naval platforms to be equipped with high performance array antennas/radars than heretofore appeared practicable.

Recent efforts have solidified the conceptual basis and provided experimental confirmation of fundamental ideas. Section II introduces some of the important concepts upon which the FOF architecture is based. Section III presents experimental results supporting the basic assumptions of the program. Section IV explores some of the ramifications of the architecture in terms of the implementation of common radar functions. Section V summarizes the contents of the report and points to the nature of future investigations. Section VI contains a set of appendices relating to particular device characteristics which might not be familiar to the reader.

II FOF SYSTEMS CONCEPT

The basic concepts behind the FOF architecture involve building blocks from two distinct disciplines, microwaves and optics. This section will discuss some of the concepts leading to a multidisciplinary design. Additional material in the appendices will elaborate on some particular building blocks.

II-1 Optical Corporate Feed

The method of implementing the equivalent of a corporate feed structure is key to the overall FOF concept. Figure II-1 shows the essence of this concept, namely, the coupling of optical beams to a two dimensional array of fibers which are in turn connected to a much larger array, the microwave antenna, after detection. The fibers sample incident optical fields and at the other end, after heterodyne detection, regenerate a microwave beam by the superposition of microwave signals from the array. In order to generate the microwave signal it is necessary to have two optical wavefronts incident on the fiber optic pickup. One is the unshifted optical carrier and the other is both frequency shifted and propagating at an angle from the first. The field at a given fiber optic cable input aperture, i, located in the fiber optic (FO) pickup plane is given by

$$E(y_i) = A_1 \exp j(K_1 \bullet y_i + \Omega_1 t) + A_2 \exp j(K_2 \bullet y_i + \Omega_2 t) \qquad \text{eqn II-1}$$

where y_i is a vector in the y plane (the vertical direction in the figure) to the i^{th} fiber, the A's are the amplitudes of the light waves, the K 's are the propagation vectors of the waves and the Ω's their angular frequencies. The fiber array samples these plane waves and connects to a larger but scaled version of the samples, the microwave array elements. The two lightwave components traverse nearly identical paths after being constrained to a fiber. The relative phase varies with distance down the fiber in proportion to the difference wavenumber between

the components. Since all other fibers map samples of the two wavefronts in the same manner, fiber lengths need be identical only to an accuracy small relative to a reciprocal difference wavenumber, i.e. as $1/(K_1-K_2) = 1/\Delta K$. This is proportional to the microwave wavelength (Λ). A detector at the antenna backplane square law detects E to regenerate a microwave field at the i^{th} antenna element proportional to

$$a \cos(\Delta K \bullet y_i + \Delta\Omega t) = a \cos(k \bullet Y_i + \omega t) \qquad \text{eqn II-2}$$

where now the spatial term is written in the antenna element vectors, Y_i. Other terms at light and doubled light frequencies do not flow in the microwave circuit. The difference terms, of wavenumber and frequency (k,ω), denote the microwave wavenumber and frequency respectively. The amplitude, a, is a function of the individual A's and the detector properties (see appendix). From this equation it is seen that the wave propagation vector created at the antenna is a scaled version of ΔK. The microwave frequency ω is the difference, $\Delta\Omega$, between the optical beam frequencies.

The antenna elements are considered to be canonically spaced at $\Lambda/2$. An equivalent spacing, $\lambda/2$, of the optical fibers is not possible. In fact, if normal diameter fibers are used, say 125μm, they are spaced some 150λ apart. For this reason a very small angle change between the incoming optical waves causes a large change in the sine of the angle of the microwave beam. From the condition that equal phase shifts occur between the optical and the microwave sample points, one can write, from figure II-1,

$$(\Delta y/\lambda)\sin\theta = (\Delta Y/\Lambda)\sin\Theta \qquad \text{eqn II-3}$$

where θ is the angle of divergence between the optical waves and Θ is the resulting launch angle from the antenna. For $\Delta y = 150\lambda$ and $\Delta Y = \Lambda/2$ one notes that

$$\sin\theta = (1/300)\ \sin\Theta$$

and a "magnification" of 300 exists in the fanning out of the corporate feed. This implies that the total angular change in divergence optically is less than 4 milliradians. (Greater divergences actually yield real quantities but a more complicated analysis is necessary.) For example, a 0.19° divergence between the two components will induce a π phase shift between adjacent fibers. This is the shift required between broadside and endfire. To a very good approximation the two optical beams propagate along the same direction, diverging at most by 4 milliradians. This has the advantage that nearly the same fiber optic waveguide mode is excited by the two waves and they can be expected to have a long correlation path in fiber. It will be noted that the two optic waves do not travel the same paths in

the fiber. Each travels an undulating path corresponding to a guided mode. The two optical components are subject to similar propagation conditions such that the relative input optical phase shifts are preserved in the microwave signals generated.

Equation II-2 indicates that the microwave array elements must be positioned in a like manner to that of the fibers although with a larger spacing. The fiber spacing would normally be that obtained by close packing a large number of fibers and polishing the ends. This leads to a hexagonal relationship of a fiber with its nearest neighbors. For a filled array small errors in the actual spacing of the fibers would not cause an appreciable error in the field at the microwave element because of the strong mutual coupling of the elements which would in effect interpolate the proper field. For a sparsely filled array however, the mutual coupling would not perform such a correction and the microwave element might have to be slightly repositioned to be in the proper place. Due to the variability of fiber diameters the lattice of input samples would be locally hexagonal but globally somewhat random. This feature could be exploited to achieve non-periodic arrays which would reduce the effect of grating lobes from the microwave array. For sparsely filled arrays where there is little mutual coupling between microwave elements, this technique is useful in suppressing variation in sidelobe level, at the cost of increasing the average sidelobe level.

II-2 Optical Beamsteering

Synthesis of an optical beam control system now devolves into a problem of creating the two variably divergent optical waves. Figure II-2 illustrates a method of creating two independently controllable plane waves. This is a Mach-Zehnder interferometer in which a rotation of either of the mirrors will change the relative divergence of the waves impinging the fiber optic pickup plane. The solid lines in the diagram represent the rays for a broadside beam. The dashed lines indicate a new mirror position and a new beam ray through the upper leg leading to a spatial phase gradient across the fiber array. Mechanical rotations limit beam switching speed but can be used in situations where very slow response is adequate.

Figure II-3 illustrates the first beamforming implementation concept which evolved in this study. It is of a Mach-Zehnder type in which a low frequency acousto-optic beam deflector (AOBD) in the upper leg scans a spot in the Fourier plane of the cell which in turn alters the arrival direction of a plane wave at the fiber optic pickup plane. The lower leg of the circuit simply offsets the light incident by a microwave frequency by use of an acousto-optic modulator (AOM). The assembly is therefore an implementation of the FOF ideas. The preference for AO (acousto-optic) modulators over EO (electro-optic) ones is due primarily to relative maturity of development. AO devices of the types required are far and away the most highly developed active, signal processing components

available to the optical designer. There are, however, a number of drawbacks to the indicated circuit. The microwave AOM cell exhibits low diffraction efficiency, exhibiting of order 10 dB throughput loss. Also, any change in the microwave frequency will dramatically shift the position of the bottom beam. Another problem is that it does not provide beam steering in two dimensions. A major objection is that it shows no method of receiving, only of transmitting. If the AO cell frequency is changed to provide the local oscillator frequency for the receive mode, beam deviation would be extreme and the system would not work.

Receive beamforming is accomplished by pre-phaseshifting the set of LO (local oscillator) signals. The relative phase shifts from the LO signals and the antenna element delays combine and transfer to the IF signal. When appropriate phase shifts are arranged on the LO to be conjugate to the time delay shifts, simple summing amplifiers are all that is needed to create a coherent array signal output for a given arrival direction.

An improved circuit is illustrated in figure II-4. Here the frequency shifting AOM is relegated to the back leg of the interferometer circuit coupling a master laser diode to a slave. As a result, the throughput reduction due to the AOM is made insignificant except insofar as the slave diode can be injection locked. Injection locking requires about 1% of the output power of a diode laser. To the right of the lasers, the forward legs, two AOBDs are used to deflect the beams and thereby control their divergence. One AOBD would suffice but two are used for symmetry and for easy extension to a 2D version. The use of two AOBDs has an advantage in a one dimensional system in that if both are driven at the same frequency (e.g. 80 Mhz) and are both operated in an upshift mode, the beam steering frequency does not appear on the radiated microwave signal because the difference frequency is used. Since the AOBDs are in excess of 80% efficient, optical losses are minimal.

Figure II-4 also shows a conceptualization of the TR module which could be used in the system. The light from the particular fiber mapped to a given array element is detected by either a PIN diode or an avalanche photodiode (APD). Since the signal level is quite low (probably not greater than -40 dBm since higher output powers would destroy an APD) a couple of amplification stages are shown to raise the signal power up to microwave mixer LO levels. A diode switch controlled by a TR logic line switches to the power amplifier for the transmit state or to the mixer for the receive state. The output of the mixer is coupled to a common IF line by use of a Lange coupler.

Figure II-4 also indicates that the AOM consists of AO cells. Figure II-5 illustrates the circuit intended. In this circuit light from the laser diode on the left is doubly diffracted by Bragg cells. By choosing the feeding points correctly it is possible to obtain a double upshift of the driving frequency with little or no output angular deviation and

no transverse beamshift with drive frequency. An alternate feeding arrangement achieves double angular deflection with no frequency change. These two designs form the basic building blocks for the FOF optical system. In the AOM form each microwave Bragg cell may have an octave bandwidth with reasonable efficiency, e.g. 1-2 GHz with 25-30 %. Thus well in excess of the requisite 1% energy can be coupled into the other diode over an octave of bandwidth. (The Faraday cell has been omitted for simplicity, see the appendix VI-2.) Consequently, the circuit should be able to perform frequency agile beamforming over an octave bandwidth. In the beam deflector configuration low frequency (TeO2) cells can be used which will operate at > 80% efficiency. Operating frequency range is not important since the angular deviations required are quite small.

It is instructive to do a light budget calculation for the above circuit in order to estimate the level of microwave signal available after the detector. In the back leg an attenuation of approximately 20 dB results from the two AO cells and reduces the available light to be injected to about the 1% required. In the forward legs each laser diode can emit approximately 10 mw of signal power. Figuring the AOBD loss at 1 dB and the beam splitter loss of 3 dB brings us to the fiber array with +6 dBm from each leg. An estimate of the power division loss when divided into a 10x10 array would be 20 dB, but only about 10% of the total light intercepts the fiber cores, a 10 dB loss. Estimating mismatch and propagation losses at 3 dB yields a light power of -27 dBm from each leg at the detector input. Using the equation for the heterodyned mixed difference frequency power from the appendix,

$$p = P_1 P_2 R^2 G^2 r/2 \qquad \text{eqn II-4}$$

with G = 30, r = 50 ohms, and a responsivity, R, of 0.5 amp/watt yields a microwave signal of -46 dBm. The effective conversion loss, p/P_1 , is 19 dB. Future arrays might need be 100x100 but improved lasers should be available with about 100 mw yielding again, -46 dBm of microwave power. This is some 65 dB above the noise in a 1 MHz band with 3 dB noise figure. Neodymium YAG lasers presently exist with these levels of power.

II-3 K-Space/Beamspace Diagrams

Figure II-6 shows a method of obtaining 2D beam deflections using two AOBDs. By the simple act of rotating one of the AOBDs by 90° it is possible to steer beams in any direction. Both AOBDs may be contained in the same leg of the interferometer. They are shown here in different legs for clarity. This can be seen if one considers the divergence of the two plane waves by the artifact of considering what would happen if a Fourier transform lens were inserted conceptually one focal length in front of the fiber array aperture. From basic optics plane waves are then brought to a focus in the focal plane. Two spots of light will be generated, see figure II-7, one

corresponding to each of the incident plane waves. The vector connecting the two spots is proportional to the projection of their difference wavenumber in the plane of the fibers and this determines the phase gradient at the microwave aperture which controls the beam direction. It is therefore proportional to the quantity ΔK in equation II-2 above. This construct can be used with any number of frequency components in the beamsteering cells and is the definition of a K-space diagram.

The solid circle in Figure II-7 on the x-axis indicates the point where light would focus for one of the waves if a lens were inserted. The x-axis is the locus of all possible positions this spot could occupy. The distance from the y axis is proportional to the deviation from the central operating frequency, e.g. 80 Mhz. A similar situation exists for the y-axis open circle. The vector connecting the two circles is related to the divergence angle or projection onto the fiber optic pickup plane, i.e. ΔK. The angle between the x-axis and the maximum gradient of phase with position is the azimuth angle and the length of the vector is proportional to that gradient. These two parameters are the natural coordinates of beamspace. In a polar plot where azimuth angle is measured from the x-axis and length of the vector is related to elevation angle, the K-space quantities can be reinterpreted in terms of the far field position of the main beam. The diagram indicates the center of the far field pattern. Other factors such as the size of the array, whether it is filled or not, etc. will dominate the actual beamspace pattern shape by a convolution of their angular spectrum with the beam center "delta" function. The open/closed circles denote the master laser light frequency and upshifted light frequency. From the K-space representation one can calculate the actual radiated frequency as the difference encoded by the two types of circles, plus the difference between the x and y vernier frequencies.

III EXPERIMENTAL RESULTS

The first experimental arrangement studied is diagrammed in figure III-1. This circuit has a potential advantage in that the frequency offset between the two legs of the modified Mach-Zehnder interferometer is obtained by sideband injection locking techniques and does not require a separate optical component (e.g. an AO cell) to modulate the light emanating from the master laser diode. Direct modulation of one of the laser diodes provides FM sidebands to which the slave laser is be locked. The figure shows the monitoring optics used in the adjustment and tuning of the laser diodes. An 8 element array of fibers was fabricated to interface to an 8 element microwave array to allow experimental verification of the proper operation of the circuitry.

Instead of actually connecting the output of the fiber array to a linear array antenna, a parallel plane microwave lens was used, figure III-2. The entire perimeter of the "D" section is filled with coaxial probes. Probes not attached to a

transmission line are terminated in a matched load. This lens locates a series of input ports on a circular locus relative to the central output port on the straight side of the "D". Radiation inside the parallel plane region is entirely absorbed either by the terminations or by the output transmission line. When the RF phase front is altered, a new beam direction is generated. By using the central output probe, the scanned pattern from the array, the array factor, may be measured. This pattern is not the same as would be measured for a linear array because the field probe does not change angle, it only measures the phasor sum of the radiation from the probe array and as such is not influenced by the element patterns nor the diminished projected area of the array at high angles from broadside. Phase shifts from element to element can progress to large multiples of π radians replicating the scanned pattern with period 2π. This is called the phase scanned pattern or the array factor.

This experimental arrangement did not work well because of the effects of carrier feedthrough in the slave laser leg. Although the slave was locked to a sideband, the frequency unshifted light component from the master laser occurred within the passband of the slave. So instead of having only one lightwave component in the output of the slave laser there were two, one at the master laser frequency, Ω, and one at $\Omega+\omega$. These generate multiple beams from the probe array from intermodulation products. To alleviate this problem recourse must be made to a circuit generating only a single lightwave component in each leg. Although the experiment did not succeed in generating a 3.2 Ghz signal with good spectral purity, the experiment did show that for frequencies above about 6 GHz this would be a viable procedure. At this frequency offset there would be sufficient carrier rejection to yield signal purity of the magnitude required.

Figure III-3 illustrates a modification which yields high spectral purity. A single microwave Bragg cell is inserted between the master and slave diodes. In essence it operates in a single sideband, suppressed carrier mode since the undeviated master laser light will not focus into the semiconductor laser junction and will not influence the output light from the slave. It was observed that a change of operating frequency of 1 MHz shifted the sideband out of the proper geometry to inject significant power into the laser junction and the system would then not injection lock. The use of a doubly diffracted beam undergoing no angular deviation but twice the frequency shift would cure this problem and permit wideband frequency agility. The layout indicated in the figure is not optimum because the total light path from the front of the master laser and that from the back to the beam recombination point should be the same. This is because of the finite coherence length of light from lasers. Even though the feedback beam passes through a slave laser, coherence is maintained. For this experiment however, coherence did not present a problem and the arrangement indicated worked satisfactorily. It should be noted that the two AOBDs

indicated in the figure should be located as closely as possible to the lenses (not shown) which relay the light beams to the fiber array. In this way walkoff due to the beam not propagating in the direction of the optical axis may be minimized. Walkoff is unavoidable in this architecture and since it alters the overlap of the two beams at the fiber optic pickup plane it must be accommodated in the optical design.

Figure III-4 shows the results using a single fiber of the array. As the AOBD drive frequency ranges from 25 MHz to 105 MHz the power level sensed at the output shows a fairly symmetric variation. This range is well in excess of the transducer bandwidth and is therefore attenuated severely at band edges. The rolloff is due to the combined effects of beam walkoff and transducer efficiency. This information was taken using a network analyzer so the actual phase of the output was also available. By repeating these plots for all the fibers it was possible to adjust the magnitudes and phases to be nearly identical. Magnitudes were adjusted by varying the gap between the end of the fiber and the sensitive area of the APD. The phase was altered by trimming the length of fiber at a splice.

Figure III-5 shows the total response when 7 fibers were combined using the microwave lens. One of the amplifiers had failed limiting the array size to 7 for the experiment. The five largest peaks correspond to a situation where the output of the fiber-detector combination drive all elements in phase. There is then a 2π phase shift between major peaks. Their magnitudes are modified by the AOM-aperture frequency response, i.e. walkoff. The fine scale peaks are sidelobes and show rather severe phase errors caused by misalignment of the optics during this particular run.

Figure III-6 shows the final array factor pattern obtained. Both theory and experimental results are shown, the theory being that of 7 phasors with a linear progression of phase shift with equal weights. Although theory and experiment do not agree exactly, the agreement is quite good. It is only through this agreement that the abscissa scale can be accurately set. The natural scale is frequency into the AOBDs and a measure of phases would require breaking the transmission line. But the agreement with theoretical shape allows an identification of the frequency change for 2π phase shift thereby giving the conversion factor between frequency change and phase gradient. The magnitude disagreement at $\pm 2\pi$ phase shift is caused by the rolloff in the AOBD-aperture frequency response. The null positions do not seem to occur in exactly the correct place but that is due to non-linearity in the sweep frequency source used in the experiment. Of most significance in terms of the level to which errors in magnitude and phase have been reduced is the null depths, $\geq$ 27 dB below the peak response. The depth of null is indicative of a 0.5 dB rms power imbalance or a 3° rms phase variation at the 7 elements, or some intermediate combination of smaller rms errors.

IV MULTIPLE BEAM FORMATION

The extremely simple method in which the FOF is made to form beams, namely, by the selection of drive frequencies into two AOBDs, inexorably leads to the question of pattern synthesis. By this we mean methods of perturbing the quiescent antenna pattern to achieve some particular result, usually that of placing a null in some direction from which jamming is expected or observed (open loop vs closed loop). By diminishing the light beam intensity at the edges of the fiber optic pickup by apodization, by inserting multiple frequencies into the AOBDs, or by creating additional beams in any way in the optical subsystem, the radiation pattern may be modified.

IV-1 Dependent Beams (Pattern Synthesis)

Figure IV-1 sketches a modification to the optical system which can add an additional, parasitic beam to the main pattern. An additional beam is generated by splitting the light in the upper leg and routing it through another AOBD, reflecting it from a mirror which can be rotated about two axes, and then recombining with the main beam. The fraction of light extracted may not have to be considerable since this technique would probably try to place a null in a far out sidelobe and hence requires only a small fraction of the light that the mainbeam does. To get independent control of the far field pattern from this parasitic circuit, the phase, amplitude and beam direction (4 parameters) must be available. Figure IV-2 shows the K-space diagram for this situation. It shows the two basic mainbeam frequencies and the parasitic beam which can occur at any point in the diagram because of the arbitrary Θ,Ψ available from the mirror tilts. The intermodulation term between the solid black circles will not occur in the RF passband and can be ignored. With the proper adjustment of the amplitude (drive power in the AOBD) and phase (phase of the drive signal) this component can be made to create a null. Parasitic beams can be formed in a number of ways in the optical subsystem in order to have a multiplicity of nulls controlled by the system. All must however be created in the same leg of the interferometer.

Consideration of the circuit in Figure IV-1 and the nature of the K-space to beamspace relationship will show that the angles Θ,Ψ are "attached", albeit somewhat loosely, to the main beam direction. As the main beam direction is altered the parasitic beam moves also to maintain nearly the same direction relative to the main beam direction. Were it not for the non-linearity in the mapping from θ to $\cos\theta$ a change in beam direction would carry the parasitic beam along exactly. Due to this and the fact that the farfield pattern is modified depending on the look direction by both the element pattern and the aperture projection in that direction, the parasitic beam will not maintain a correct set of parameters (Θ,Ψ,A,φ) to maintain a global null. Further since the parasitic beam is probably attempting to create a null in the far-out or random sidelobe pattern region the requisite phase and amplitude is not known a

priori, nor is it constant with look direction. It is thus necessary to search for a null. This means closing the loop in some manner, either by correlating with another antenna beam (beamspace cancellation) or by operating on receive only and searching θ,Ψ,A,φ until a null is obtained. This 4D search may not be well behaved and a better strategy might be to keep θ,Ψ fixed as determined by open loop procedures and searching only A,φ in the sidelobe region.

Another method of creating additional dependent beams is to drive the AOBDs with multiple frequencies. This will lead to a monopulse beamformer. Consider the K-space diagram in figure IV-3. Each of the AOBDs is driven by two frequencies. Of the 6 intermodulation products possible two occur at IF and can be ignored in the RF beam formation considerations. The 4 remaining beams are organized as shown in the beamspace part of the diagram. It will be noted that such a cluster of beams can provide beam sharpened behavior if the signal to noise is high enough and the beam responses can be separated. Figure IV-4 shows the situation for a normal monopulse situation and the FOF equivalent circuit. Reference to IV-3 will convince that each of the beams though occurring at RF has a distinct IF frequency because of the vernier frequency required in the beamforming circuitry. The use of a frequency channelized IF receiver will allow separation of the beams such that sums and differences can be made in exact conformity with the classic monopulse processor. After channel separation all the channels must be translated to a common center frequency.

It will be noted that uniform weighing of the signals is a key factor in the synthesis of the monopulse cluster. Attempts to use non-uniform weights for a more general multibeam purpose generates unwanted parasitic beams. With non-uniform weights, say A_x ,A_y for the main beam and b_x , b_y for a second beam ($b<<A$), the cross product terms like A_x b_y have a weight intermediate to A_x A_y and b_x b_y and are therefore a severe perturbation. Additionally terms like A_x b_y have a limited range of positioning relative to the main beam and so this approach appears to be of limited utility in sidelobe cancellation.

IV-2 Independent Multiple Beams (Anti-jam)

The procedure scoped in section IV-1 for the modification of the far field pattern by creating additional plane waves in the optical subsystem (manipulation of the K-space diagram) can not be extended to obtain independent multiple beams. To create closed loop beams eliminating the effects of interfering signals feeding through the sidelobes it is necessary to have access to separate channels. This is referred to as a beamspace method of anti-jam. It exploits the nearly orthogonal set of beams possible from a many element array. It is necessary to form as many auxiliary beams as needed to assign a separate beam to each jammer. Each receive beam signal then strongly weighs a given jammer waveform with only weak contributions from

other sources. A cross-correlation with the main channel then establishes the approximate weight required to use in extracting or cancelling that jammer from the main signal channel. The set of waveforms, main plus set of auxiliaries, can be input to a canceler circuit (e.g. a Gram Schmidt) to maintain radar performance in a multi-jammer environment.

Figure IV-5 shows a diagram of one hardware modification which implements beamspace anti-jam using an FOF architecture. The main modification is a replication of the control subsystem and adding receiving units to the TR module. A multiplicity of receivers accesses simultaneously and independently a number of individual beams. The figure indicates the TR module required to do this. Corresponding receivers at each antenna element TR module are driven by an optical control subsystem which generates a phase steered LO signal feeding the microwave mixer. This then extracts different Fourier components from the phase projection onto the array, thereby accessing different beams in space. Only one of the chains includes a transmitter (another chain could be coupled in to permit spoofing). Subsequent to the IF combiners the individual receiver channels are routed to the signal processor where cross correlation properties are estimated and eliminated from the final weighted result. This does not generate additional transmit beams but does generate a multitude of receive beams. Each of these beams might require patterr ynthesis to further (beyond basic pattern rejection) reject c .er jammers. In this way, the near orthogonality of beams may be further improved.

An alternative exists to increasing the TR module complexity. This alternative obtains multiple beam performance by providing additional optical beams. K-space diagrams for cases using decoupled K and Ω (beam deflection without frequency shift, frequency shift without beam deflection) involve no vernier frequency shifts. One of the beams, usually the reference beam, is taken as the origin and can without loss of generality be assumed to propagate along the optical axis of the system. The microwave frequency is given by the difference frequency between the beams while the phase gradient is simply the projection of the steered beam onto the plane of the fiber array. Figure IV-6 illustrates a general case. This circuit excites a large number of beams simultaneously. All of the slave laser diodes are locked to the master laser and each beam path passes through a pure AOM and a pure AOBD. Combining through half or partially silvered beam splitters allows all the beams to be superimposed on the fiber array. The four fiber subarrays shown on the right are optically overlaid to synthesize an array with four times the number of samples with half the effective interelement spacing in each dimension. The relay optics are not shown for simplicity. The microwave input for each of the beams is to the AOMs and the independent beam steering frequencies is input to the AOBDs. Shown in the lower right hand corner of the diagram is the K-space diagram for this case. Four independent beams are shown, each with a different azimuth direction and a

different elevation direction. Each can also operate on a different RF. The range of microwave frequencies must be less than an octave to avoid difference frequencies from different beams generating in-band signals. To receive the transmitted signal using the synthesized pattern, the mixer in the TR module is driven with the same controls but frequency shifted by the offset required to downconvert (or upconvert) to the IF band. The proper phase gradients will exist to filter out the separate signals and relocate them to their desired IF.

One difficulty with this procedure is that the mixer in the receive leg of the TR modules sees a set of distinct local oscillators. The time waveform is the Fourier transform of this spectrum and could, for certain possible sets of local oscillator tones, be a repetitive narrow pulse. This would cause no problem for a linear system (filters work this way) but for a nonlinear mixer, driven very hard to achieve minimal conversion loss and maximum dynamic range, the conversion loss could be expected to be increased, sometimes very considerably.

IV-3 Time Dependent Beams (Chirp)

Figure IV-7 shows a time dependent beamforming case. This diagram is intended to beamform using chirped radar waveforms. Because of the intrinsic dispersion of a phased array antenna, a change in the RF will squint the beam, see appendix VI-4. By synchronously changing the AOBD control frequencies, as indicated, a constant beam direction in space can be maintained. Although one of the vectors on the left in figure IV-8 is longer, the effect of increased RF causes it to shorten in proportion to the change in operating frequency upon transfer to the beamspace diagram. (Note that the spot on the y-axis designating the light frequency is further encoded to indicate the change in frequency.) If the AOBD chirps are chosen correctly the beam pointing direction does not change. This allows the entire broadband waveform to be directed at a target and thereby avoid a waveform filtering arising from pattern squint. A similar discrete beam switching is effective with frequency hopped waveforms.

One of the most accurate methods of reducing radar clutter with moving array antennas uses the displaced phase center array (DPCA) concept. Here one switches between subarrays to obtain two separate returns with all radiating and receiving elements in exactly the same position. A subtraction of the two returns then cancels all fixed returns while giving a "dipole" signature for moving targets. Such switching can be incorporated in an optically fed array by the act of shifting the fiber pickup array illumination appropriately. This can be accomplished in a number of ways either mechanically (by mirror rotations) or electrically (by AO cell drives). Under-illuminating the fiber pickup array allows optical beam displacements to shift the microwave radiating aperture from one subarray to another. Such beam displacements can be effected by simply adding an additional x deflection AOBD, say, in the y deflection arm of the beam

deflection circuit. Then the x subarray addressed is purely a function of the difference in frequency of the x deflection cells. In this manner the DPCA subarrays can be electronically addressed and the DPCA algorithm implemented. Because of under-illumination the amplitude weighing would likely be of a gaussian nature leading to a low sidelobe antenna pattern.

IV-4 True Time Delay Beams (Wideband)

True time delay behavior of an array can be obtained in a direct manner by treating the wide spectral band as independent subbands as discussed in figure IV-6, see figure IV-9. Here the K-space diagram would show all the vectors pointed in the same azimuth direction but having slightly different phase gradients (wavenumber projections) to match that required to launch or receive signals from the desired direction. This is not a frugal method of using the available number of total beams however and may result in considerable conversion loss in the receive mixers (see last paragraph of section IV-2).

A far more elegant method would use the circuitry illustrated in figure IV-10. Two beam ports are required, 1 and 2, which attach to the frequency translators of figure IV-9 in beams 1 and 2. The desired pulse, scaled in frequency, would be split and passed through discriminator circuits, one with a positive slope and one with a negative. This would create two waves impinging the fiber optic pickup plane in addition to the reference. If a sinusoid at frequency 1 were applied to the circuit, beam 2 would have weight zero and the gradient which must be established by the beam deflector is that to send frequency 1 in the desired direction. The converse argument would apply if only frequency 2 were applied. If a frequency intermediate to the two band edges were applied both beams would be excited but with a weighing determined by the discrimination circuitry. Since both beams would be excited at the same frequency with only the amplitude weighing being different, an intermediate effective plane wave would be generated. Because of the small angles on the optical side of the circuit the interpolation is linear and the proper phase gradient is established to transmit each Fourier component in the direction desired.

The discriminator circuit can be built using either microwave or optical techniques. A particularly simple optical method would use an AOBD for the input of the RF signal and a Fourier transform lens to gain access to the spectrum of the signal. If no operation is performed on the spectrum and all the light from the AOBD is allowed to fall on a detector, the input signal, somewhat attenuated, is reconstructed. By putting a mask in the frequency plane of the circuit, generalized filtering can be accomplished. In particular a mask which has a variable transmittance can be used to create a discriminator whose output amplitude is a linear function of microwave frequency. By reversing the slope of the variable transmittance, the opposite discriminator can be constructed. One could also use microwave

filters. The out of band response of a multipole filter can be used to synthesize the requisite discriminator behavior, the low pass response for one of the circuits and the high pass response for the other. The main problem with the microwave solution is that the delay through the circuit as a function of frequency is difficult to keep constant.

The time delay properties of this circuit can be seen by considering the signal which results from superimposing two plane waves of the same wavenumber magnitude but different propagation directions. Obviously one has to get interference since this is the basis of the classic Lloyd's mirror experiment in optics. In equation form one has

$$a_1\mathrm{Cos}(\omega t+\varphi_1) + a_2\mathrm{Cos}(\omega t+\varphi_2) = N\ \mathrm{Cos}(\omega t+\varphi)$$

where the amplitudes on the left are related by the response of the discriminator circuits, i.e. $a_1 = 1 - a_2$, and where the subscripted phase terms are just $\mathrm{KySin}(\theta_i)$. Applying elementary trig transformations one can evaluate N and φ as

$$N = \sqrt{(((a_1\mathrm{Cos}(\varphi_1)+a_2\mathrm{Cos}(\varphi_2))^2 + (a_1\mathrm{Sin}(\varphi_1)+a_2\mathrm{Sin}(\varphi_2))^2)}$$

and

$$\varphi = \mathrm{Arctan}((a_1\mathrm{Cos}(\varphi_1)+a_2\mathrm{Cos}(\varphi_2))^2/(a_1\mathrm{Sin}(\varphi_1)+a_2\mathrm{Sin}(\varphi_2))^2).$$

The amplitude terms, a_i, are functions of operating frequency only whereas the phase terms are a function of the position in the array and the two design frequencies involved in the discriminators. The expression for N shows the required interference effect. A numerical examination of the resulting phase term shows it to be a linear function of operating frequency and element position with only weak quadratic errors (and even weaker quartic and higher terms). Such errors can be compensated for in the optical circuit by introducing opposite spherical curvature of phase front by movement of one of the lenses.

The linear phase shift introduced on the frequency components performs the necessary operation to allow broadband beamsteering. Define

$$\overline{s_o(t)} = S(\omega) \qquad \text{eqn IV-1}$$

where the overbar is used to denote the Fourier transform operator and the subscript denotes the fiber under consideration. To have time delay performance the signal at the i^{th} fiber should then be

$$\overline{s_i(t)} = \overline{s_o(t-\tau_i)} = \exp(j\omega\tau_i)\ S(\omega) \qquad \text{eqn IV-2}$$

This expresses the fact that the Fourier transform of a time delayed version of a signal is a linear phase shift of the spectrum. In an optical system the signal at the i^{th} element is given as

$$\overline{s_o(t)\ \exp(jy_iK_p)} = \exp(jy_ik_p)\ S(\omega) \qquad \text{eqn IV-3}$$

For time delay performance to result the terms in the exponential must be identical. The gradients can be computed by equating the phase shift between elements on the fiber side to that on the antenna side, namely

$$\begin{aligned} y\ K_p &= Y\ k_p \\ y\ K \sin(\theta) &= Y\ k \sin(\theta) \end{aligned} \qquad \text{eqn IV-4}$$

where subscript p denotes projection into antenna or fiber optic plane. This yields

$$\tau_i = Y_i \sin(\theta)/c \qquad \text{eqn IV-5}$$

if

$$\sin(\theta) = \Delta Y\ \omega \sin(\theta)/\Delta y\ \Omega \qquad \text{eqn IV-6}$$

where ΔY is the antenna element spacing and Δy is the fiber spacing. The discriminator circuit performs the correct operation for creating apparent time delays without introducing delay lines. The apparent delay comes from the progressive phase shift with frequency introduced by the optical system. By superposition a pulse whose spectrum is contained in the discriminated frequency interval could be expected to be launched in the proper direction.

The effects of the interference caused by the two inclined optical plane waves of the same frequency (but of generally different weights) modifies the pattern to be expected from the antenna. The sinusoidal modulation across the aperture results in two vestigial beams being superimposed on the desired beam. These are similar to range sidelobes encountered in pulse compression. They appear in the directions representing the limits of dispersion if only the center frequency of the pulse spectrum were directed correctly. They evidence the linear taper of the discriminator on the spectrum radiated in those directions. They can be expected to be of order -13 dB relative to the main beam.

V CONCLUSIONS AND FUTURE EFFORTS

This report has presented in some detail concepts related to the Fiber Optic Feed program. It has shown a number of systemic properties which might be exploited to advantage in future Naval radar systems. The architecture supports a full range of radar capabilities including pulse compression, monopulse, anti-jam, beamspace adaptivity, DPCA, frequency agility, etc. and also allows wideband beamforming. Basic experiments have verified the design principles in a transmit mode. The transition of this potential capability into operational hardware could improve Naval systems in terms of weight, complexity, flexibility, maintainability, and the like.

This is because of a simpler beam control circuit which operates with global commands, the replacement of transmission lines with fiber optic cables and the elimination of phase shifters and associated digital hardware at the element level.

The major emphasis in the future must be to translate the concepts into a reasonably robust assembly whereby an experimental evaluation of all the capabilities can be made. The main questions to be resolved by this experimental venture are

1--are there sufficient controls to use components of normal reproducibility to obtain high quality beamforms,

2--can each of the conceptual uses be translated into practice, and

3--what level of performance can be obtained at the moderate level of effort to be expended on the laboratory grade implementation?

Specific concerns relate to the relatively high gain required in the TR module (> 50 dB) . In fact such gains have been demonstrated using MMIC technology (Pacific Monolithic-private communication with E.Wilson 23 Sept 87).

With a test bed assembly the potential of the architecture with conformal arrays could be experimentally assessed. It seems obvious that geometric factors may be accommodated by optical compensation, e.g. introducing spherical aberrations conjugate to the phase effects resulting from elements positioned on a spherical surface. Likewise, phase and amplitude errors due to an element being embedded in a finite array may be ameliorated.

VI APPENDICES

VI-1 Optical Detection and Mixing

Tnere is little distinction between the processes of detection and mixing as used in the optics. At the end of each fiber optic line there is a detector operating in a heterodyne mode. The current flowing in the non-linear element is given by

$$I \approx E^2 = (A_1\exp(\varphi_1) + A_2\exp(\varphi_2))^2$$
$$= 2A_1 A_2\cos(\varphi_1-\varphi_2)$$
$$\approx \mathrm{Sqrt}(P_1 P_2 /2) \cos(\varphi_1-\varphi_2)$$

for the case of two incident waves. The proportionality can be converted into an equality by multiplying by the "responsivity", R, of the diode and by any gain, G, associated with the detection mechanism (for an PIN diode G=1 whereas for an APD, G = 10 to 100). Usually there is a matching resistor, r, loading the detector to the microwave transmission line (50 Ω). Then the power flow in the transmission line at the difference frequency is just

$$p = P_1P_2R^2G^2r/2.$$

The conversion loss of the whole process is given by the ratio p/P_1. The noise performance observed after the first amplifier is essentially the noise figure of that amplifier with little added noise from the APD.

VI-2 Faraday Cell

A Faraday cell is used with laser diodes to isolate the laser oscillator from external mismatches which can modify the mode of oscillation. It uses the same phenomenology as a ferrite isolator in microwave circuits. Laser injection locking can occur at about 1% of the laser output power. If the return loss of the output of a laser is less than 20 dB, reflections can dramatically influence the lasing. The reflection sets up an external cavity so the lasing spectrum must simultaneously be a mode or eigenvalue of the two cavities, the 100 micron laser cavity and the cavity defined by the external reflection point which may be of order millimeters. Consequently, the lasing is likely to be quite erratic if there are longitudinal vibrations of a magnitude similar to an optical wavelength. Insertion of a Faraday cell isolates the lasing output from "properly aligned optics" which tend to retroreflect energy.

VI-3 Bragg Cell

Figure VI-1 sketches the acousto-optic interaction known as the Bragg interaction. An electrical signal drives the piezoelectric transducer and converts the electrical waveform into an acoustic wave traveling in the cell material. When the incident light and acoustic wave have the geometry shown, there is an efficient conversion of light from the incident light beam

into the diffracted light beam. These cells are of a 1D nature so the diffraction occurs in the plane which includes the cell length and the optical wavenumber vector. The diffracted light beam exhibits a shift in frequency by the acoustic frequency. Upshifted or down shifted signals can be obtained with equal ease. At low frequencies, 30 to 100 MHz, up to 90% of the incident light can be diffracted. The efficiencies decrease significantly with frequency. At present of order 25-30% diffraction efficiency is available in the 1-2 GHz band.

In practice there is usually weak scattering into other beams and these limit the bandwidth of the interaction. The undiffracted beam is normally spatially filtered by Fourier transform optics and a half plane stop. Whether the cell constitutes an AOM (modulator) or AOBD (beam deflector) is primarily determined by the lateral extent over which the acousto-optic interaction is designed to work. This is usually expressed in terms of the time-bandwidth (BT) product of the cell. This is the time aperture (in acoustic velocity terms) illuminated by the incident light and the 3 dB bandwidth of the interaction (in terms of input electrical frequencies). For BT of order 10 the device is an AOM whereas for BT of order 1000 it is an AOBD.

VI-4 Corporate Fed Antenna Array

The FOF architecture involves corporate fed antennas and as such there is an intrinsic dispersion connected with the beamforming. Dispersion is used to denote a frequency dependence in the beam direction. Figure VI-2 shows an idealized sketch of a one dimensional linear array fed by a corporate power divider and phase steered by phase shifters in each element path. If a linear phase progression exists across the array, a beam will be formed in a direction

$$\theta = \text{Arcsin}((\Delta\varphi/\pi)(\Lambda/\Lambda_o))$$

where θ is the angle from broadside, $\Lambda_o/2$ is the spacing between radiating elements, Λ is the operating wavelength, and $\Delta\varphi$ is the phase shift between adjacent elements of the array. As the frequency of operation is increased the beam squints toward broadside. If the phase shifter is reciprocal then both the transmit and receive beams are handled properly by the corporate divider/combiner. For the purposes of this report we also note that usually, there is a significant loss in the power division circuit so the signals are amplified before transmission by solid state amplifiers. Further, the phase shifters are usually digitally controlled so a digital bus is routed to the phase shifters. Since the beam pattern and sidelobes are very strongly influenced by the accuracy with which the phase shifters are set (modulo 2π), sometimes a lookup table is stored with the phase shifters to allow a more precise n bit approximation to account for individual variability of the phase shifters as a function of frequency of operation.

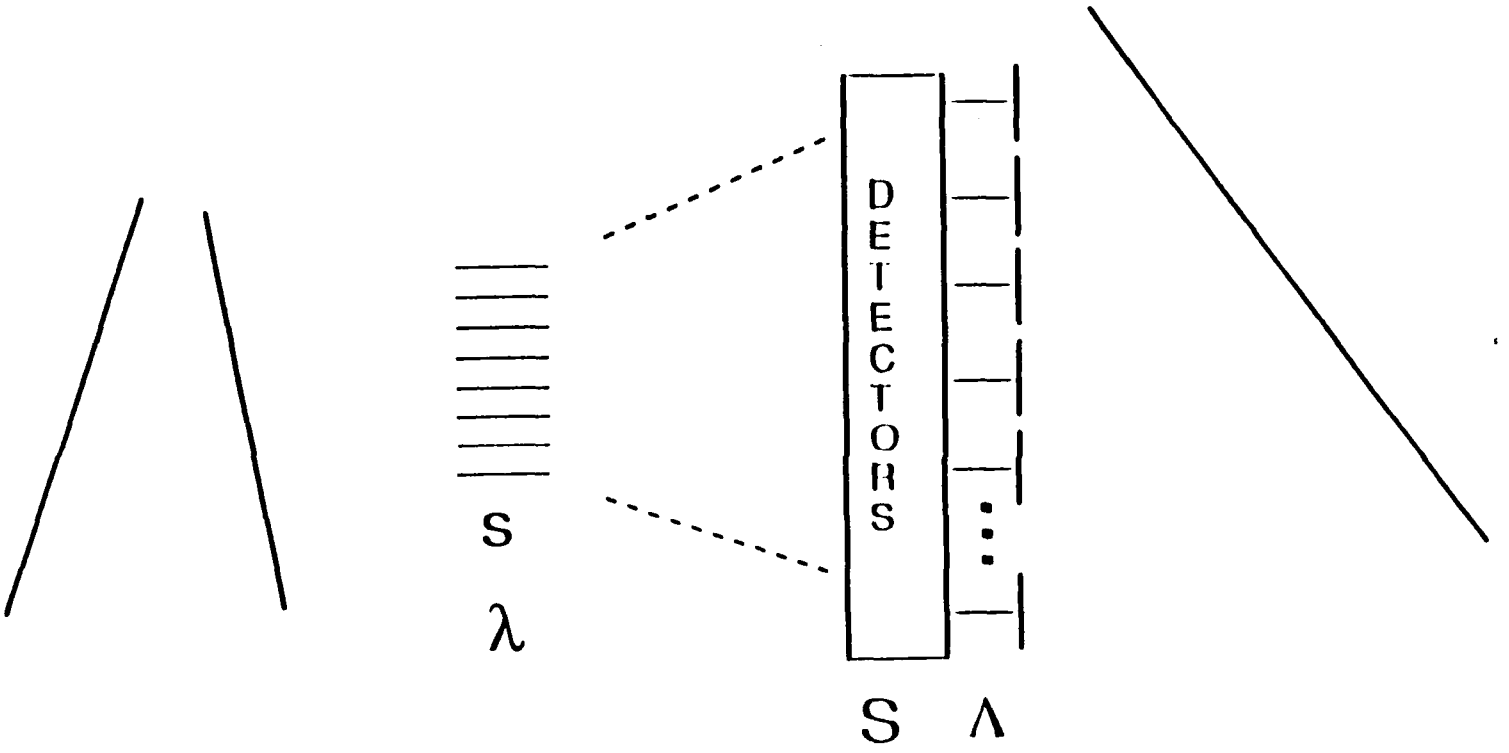

Fig. II-1 — Optical feed concept showing spatial sampling of two optical waves of different spatiotemporal characters generating a microwave beam

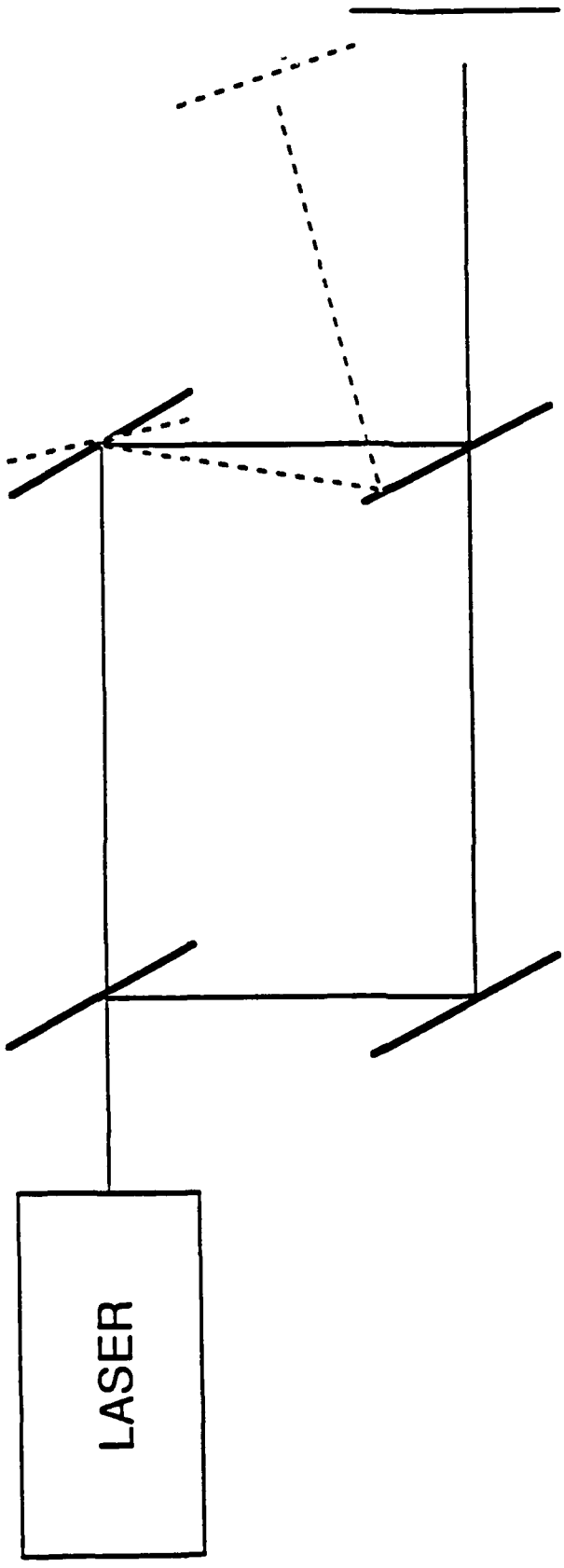

Fig. II-2 — Mach-Zehnder interferometer method of synthesizing two independently controlled beams

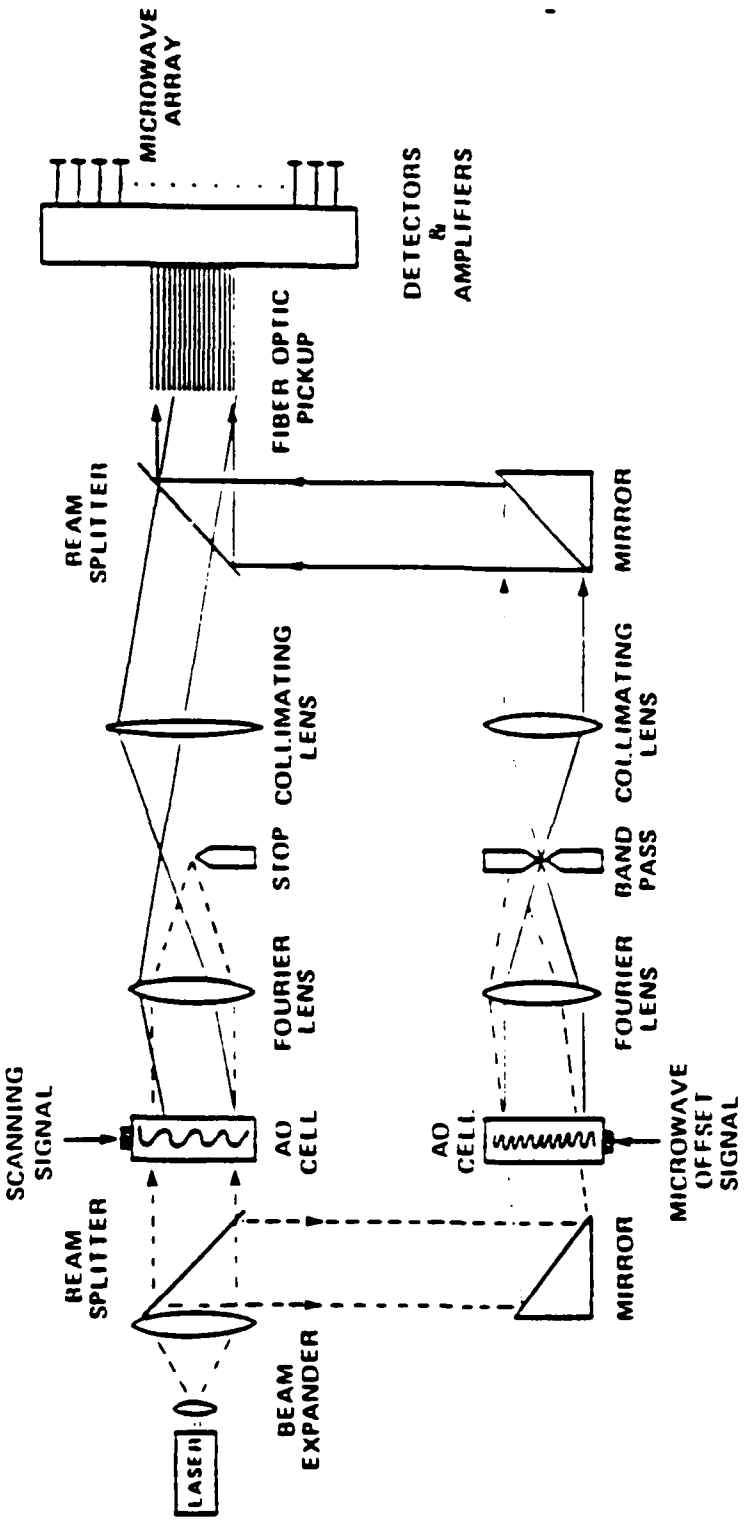

Fig. II-3 — Interferometer with AO cells capable of generating scanned microwave beams

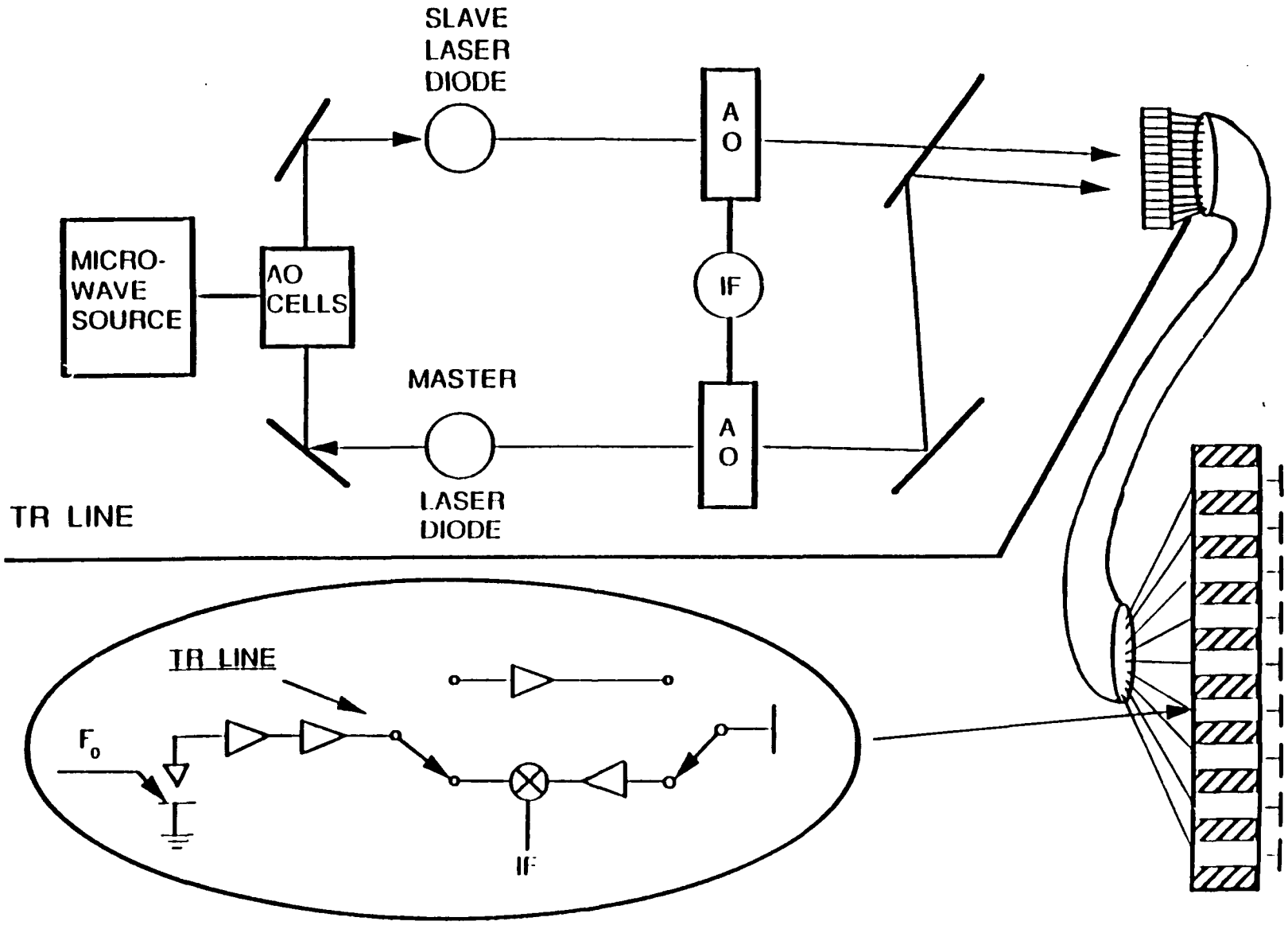

Fig. II-4 — Practicable systems concept for fiber optic beamforming showing TR module

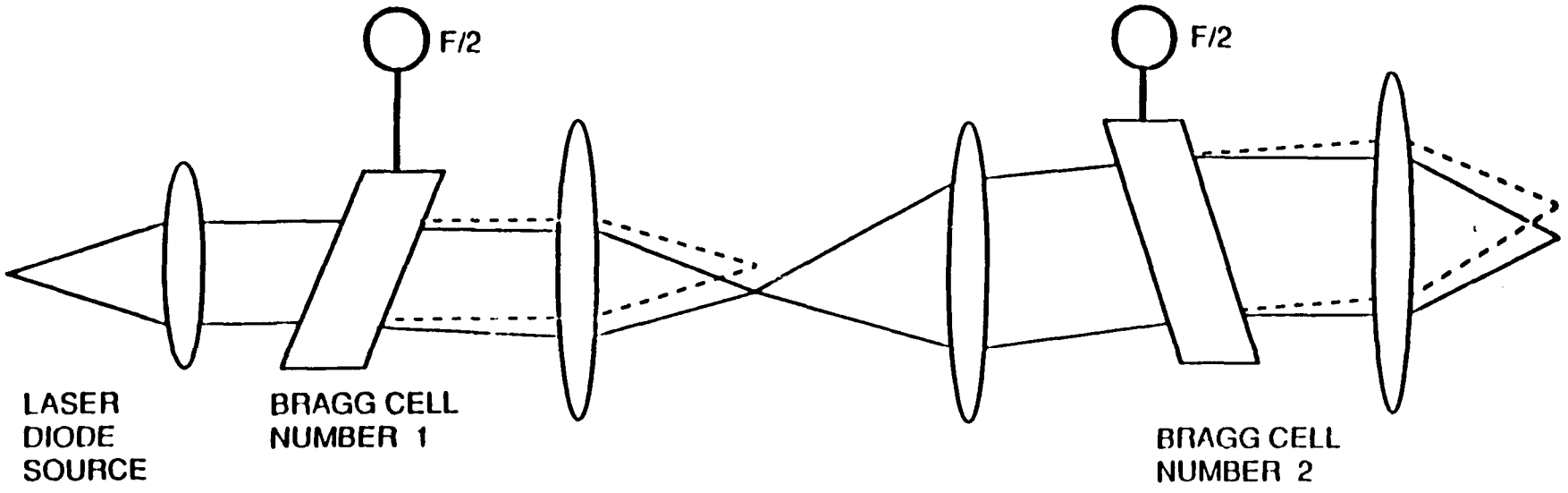

Fig. II-5 — Dual Bragg cell system to perform frequency translation without output beam tilting

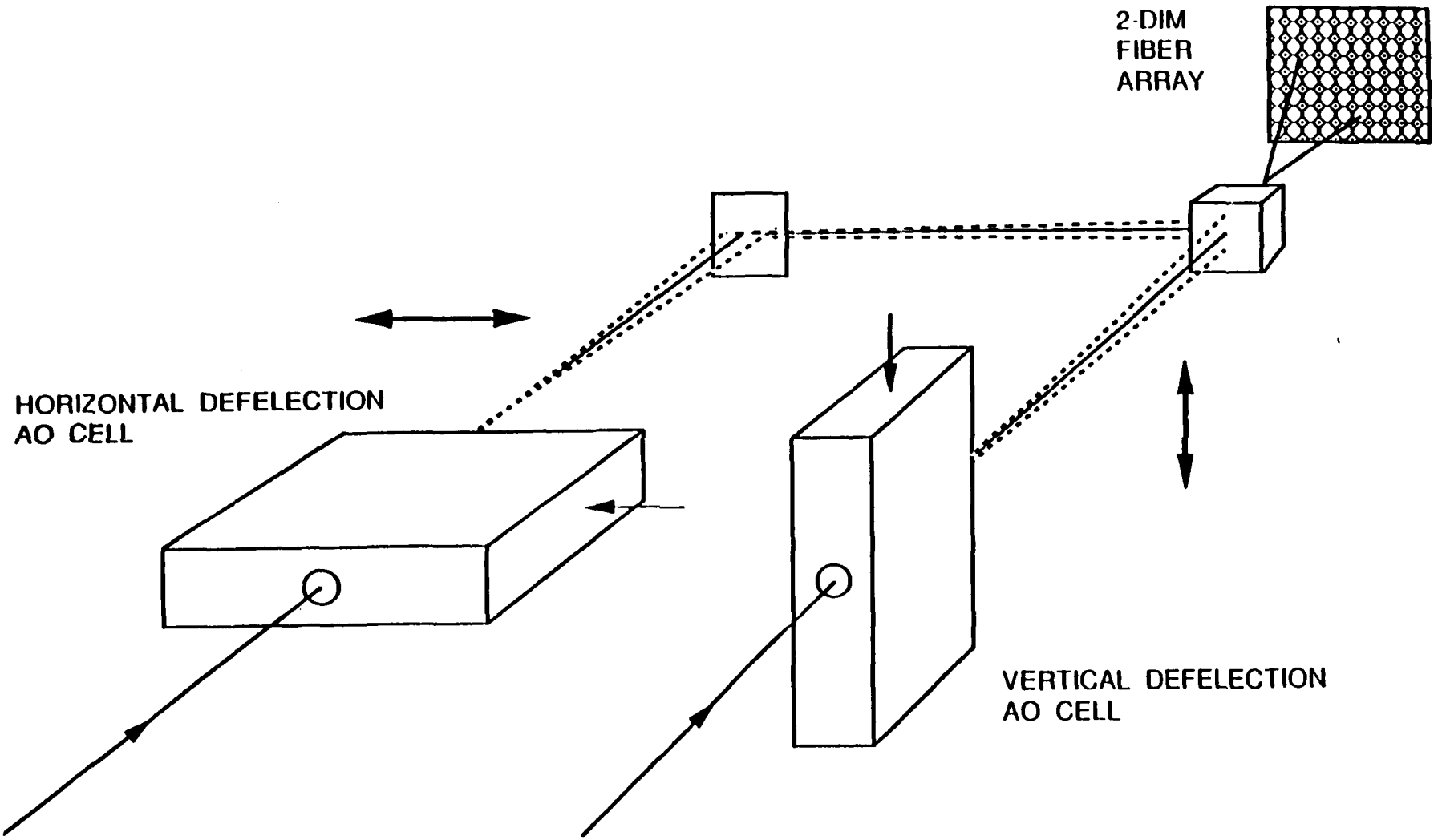

Fig. II-6 — Two dimensional scanning using crossed AO cells

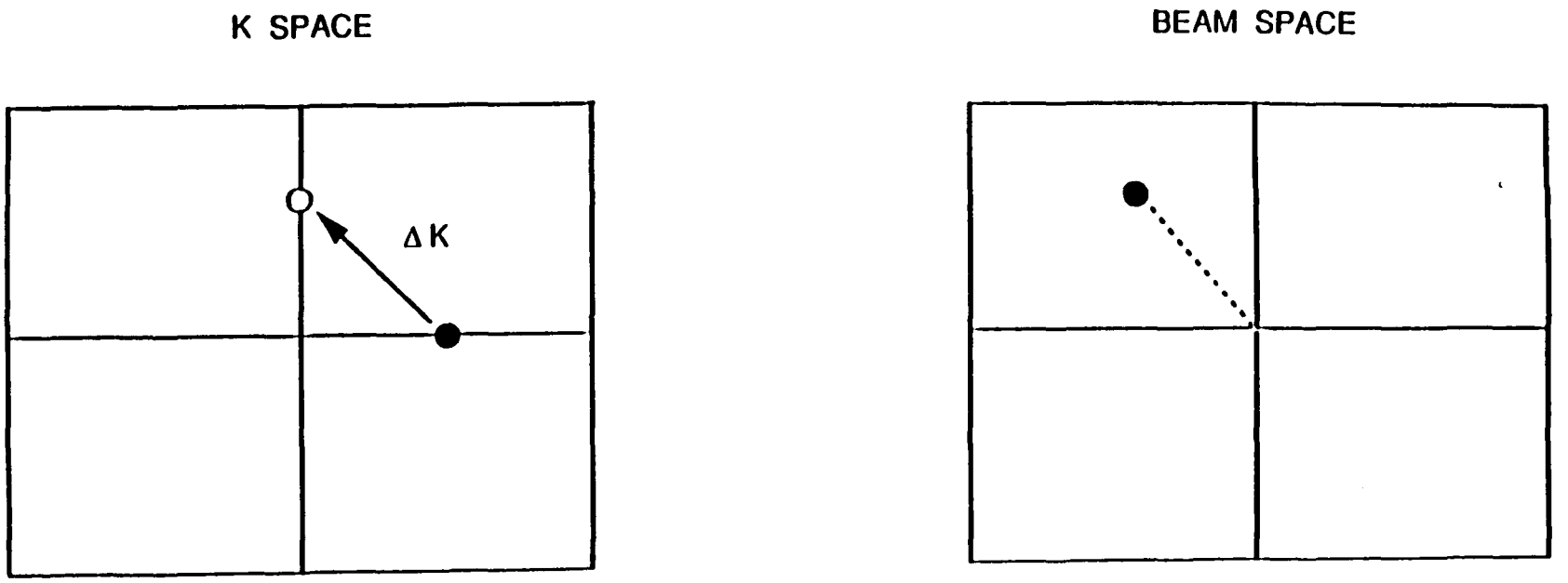

Fig. II-7 — K-space and Beamspace diagram

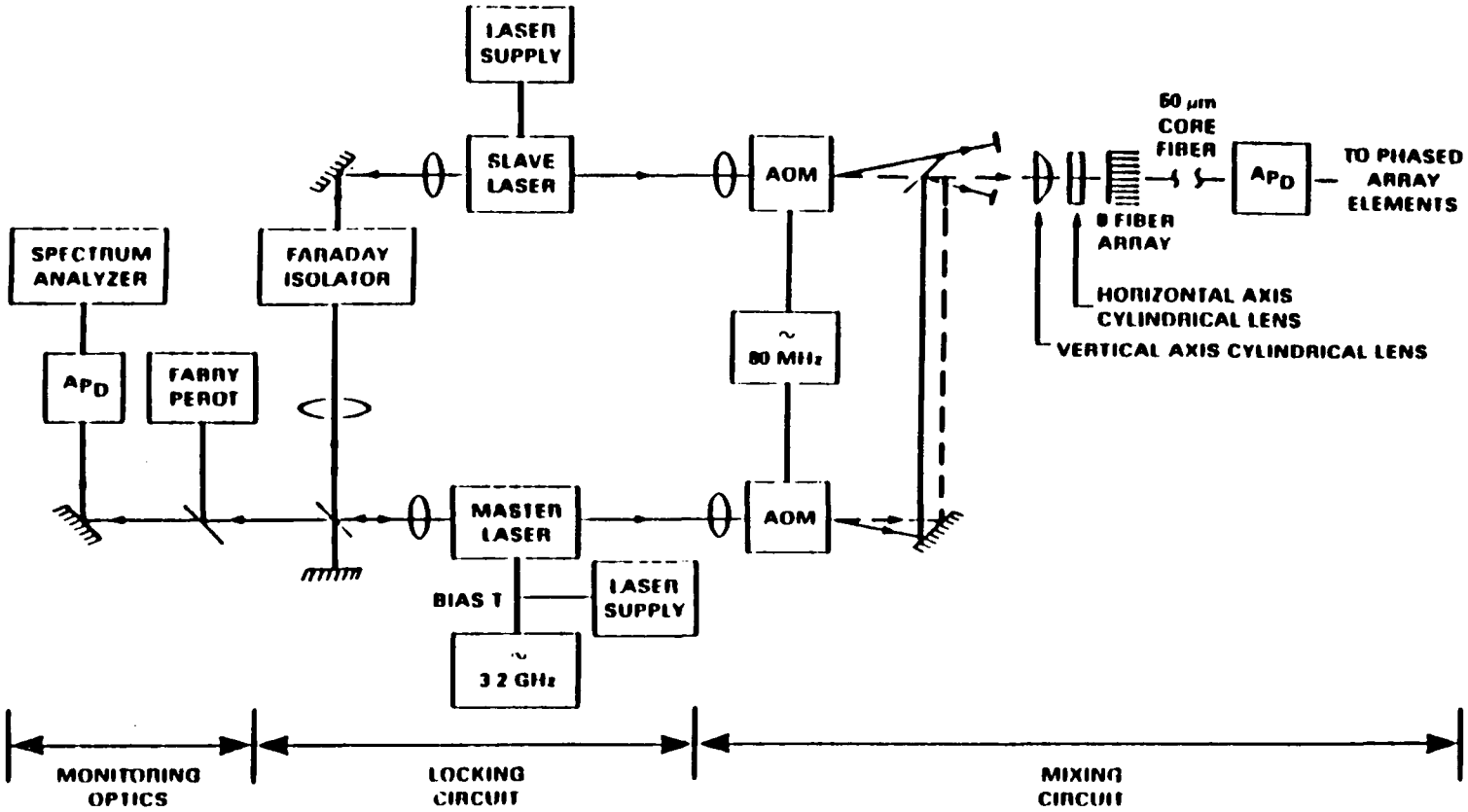

Fig. III-1 — Injection locking approach to fiber optically fed phased array

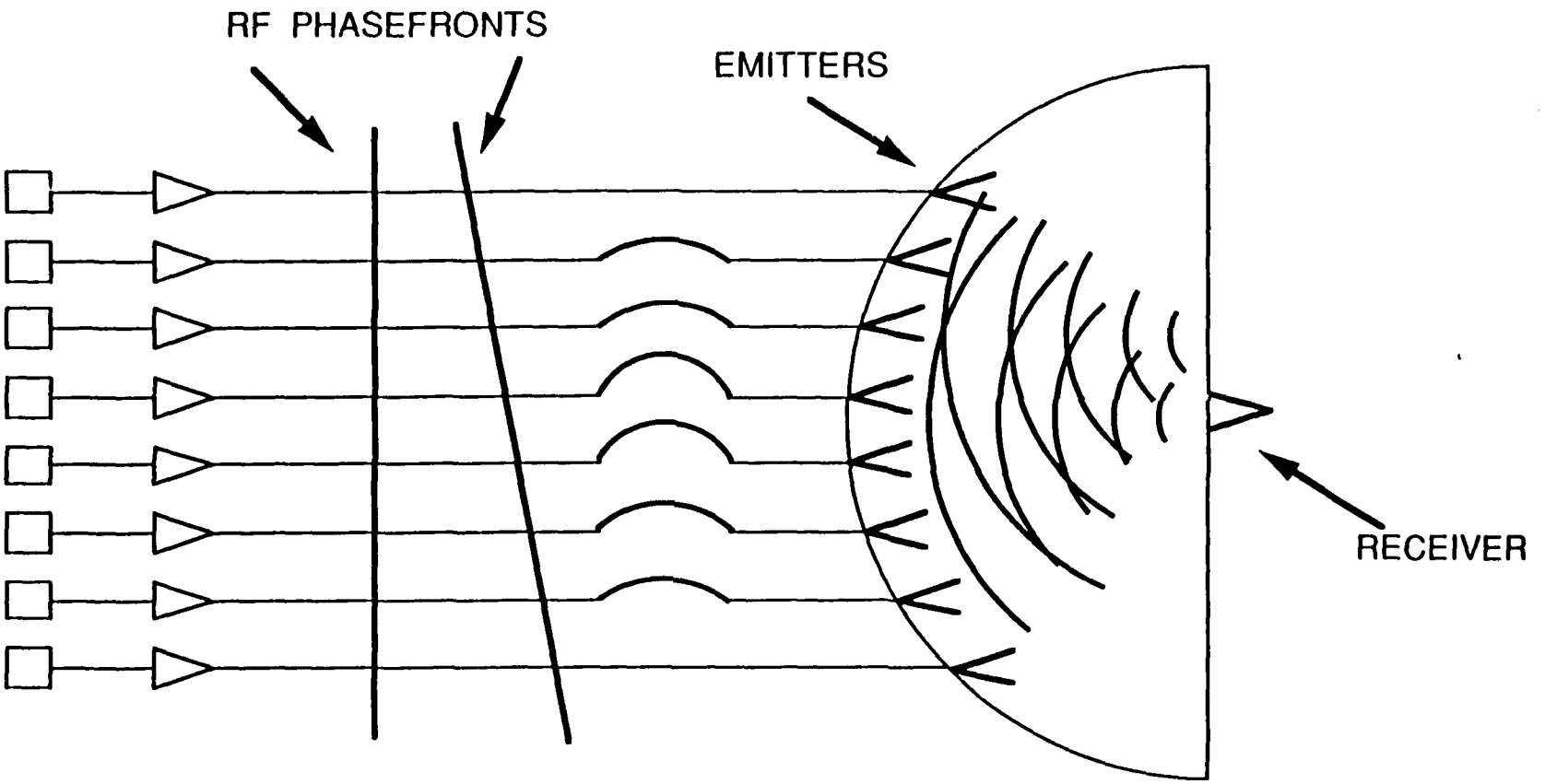

Fig. III-2 — Array of detected and amplified microwave signals driving a microwave lens to allow determination of array factor pattern

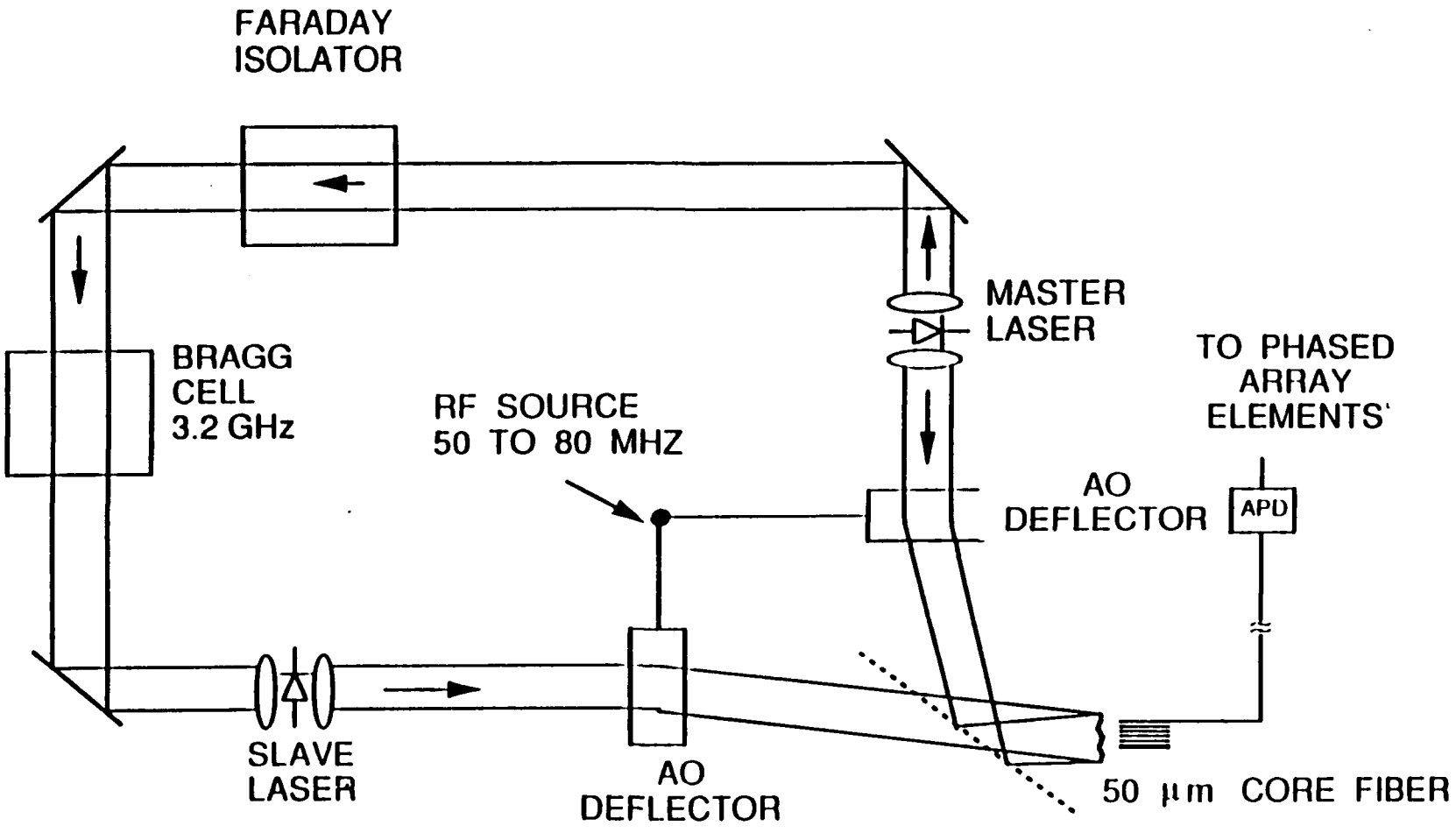

Fig. III-3 — Modified MZ interferometer yielding high spectral purity in the regenerated microwave signal

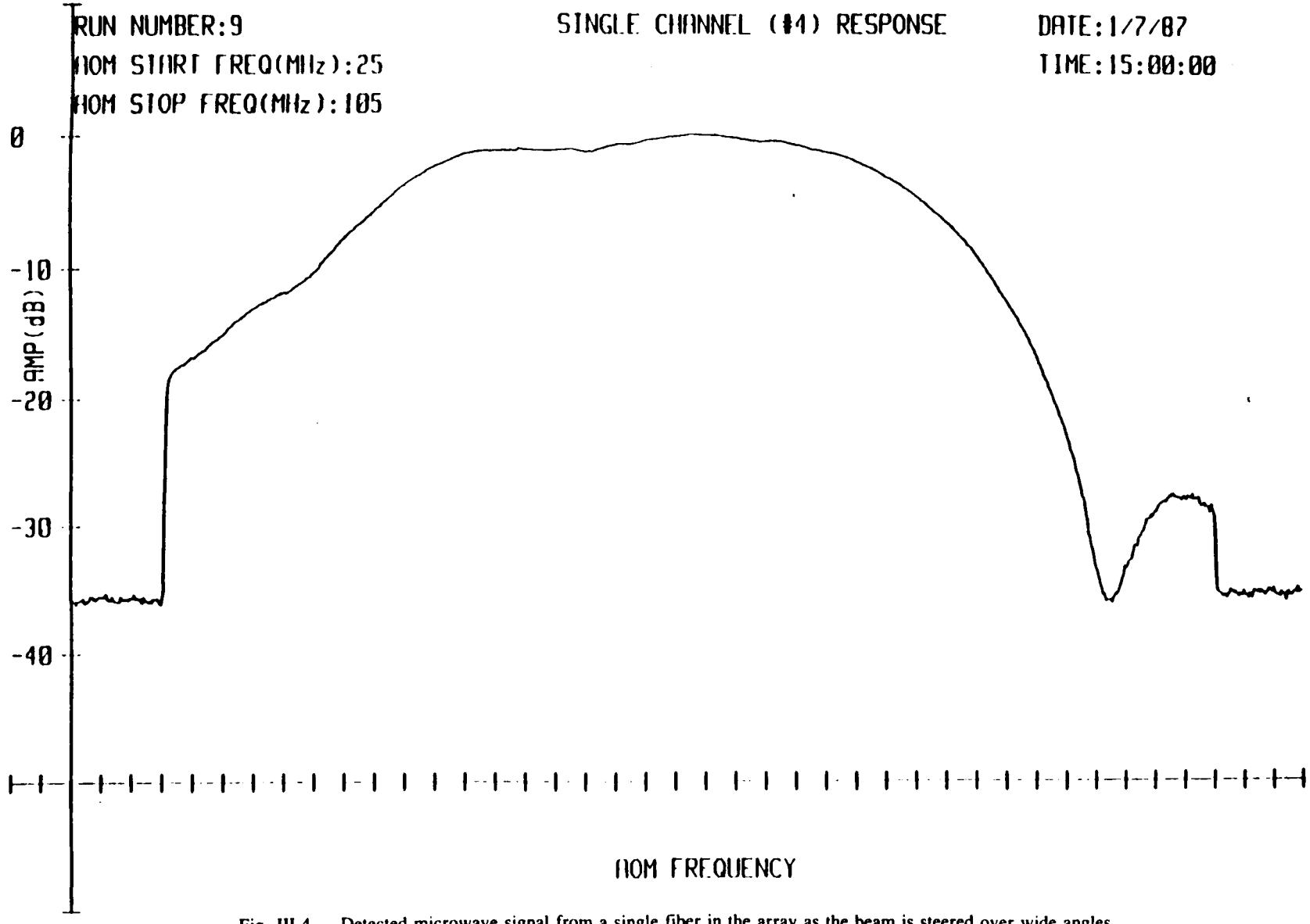

Fig. III-4 — Detected microwave signal from a single fiber in the array as the beam is steered over wide angles

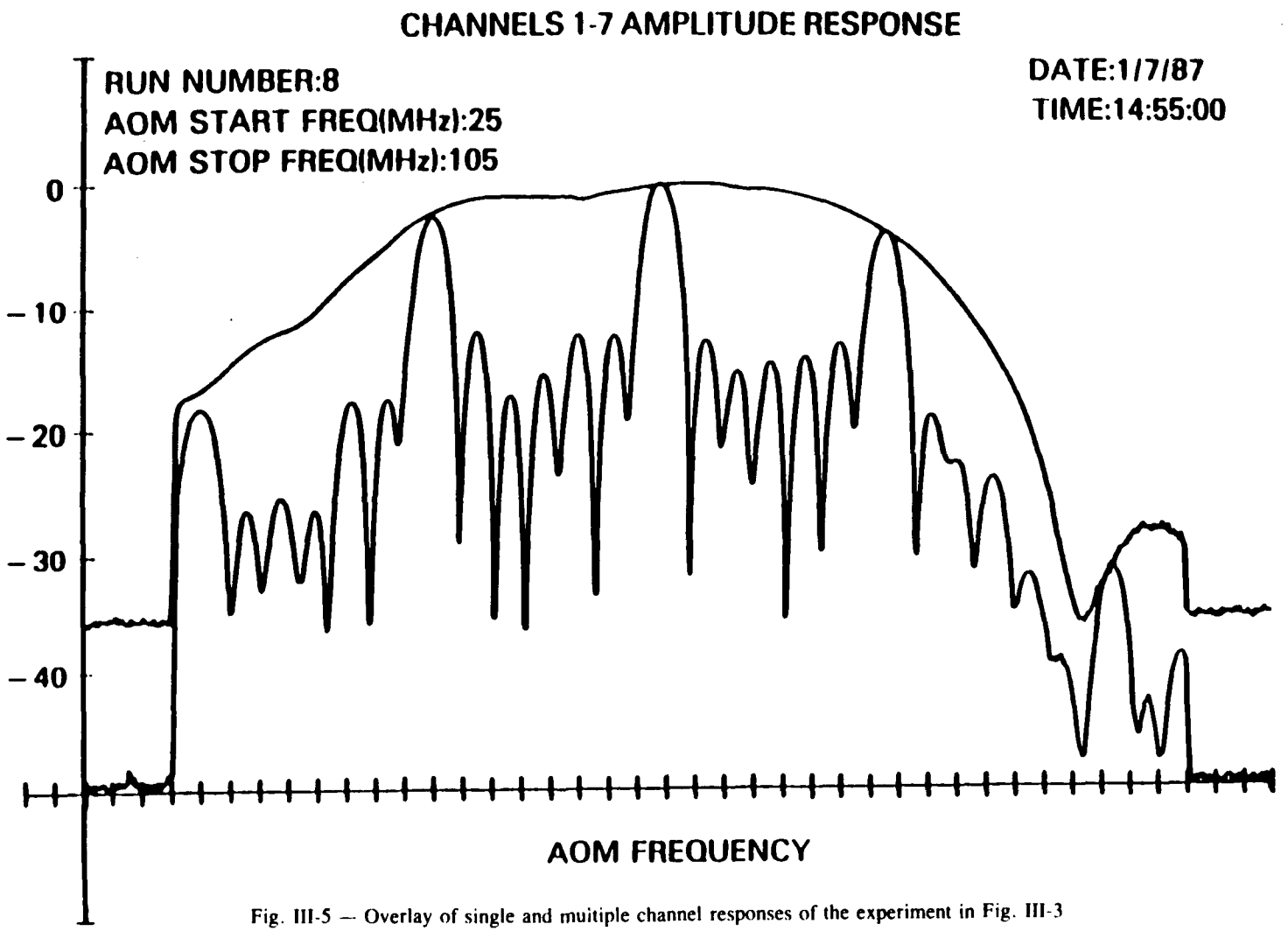

Fig. III-5 — Overlay of single and muitiple channel responses of the experiment in Fig. III-3

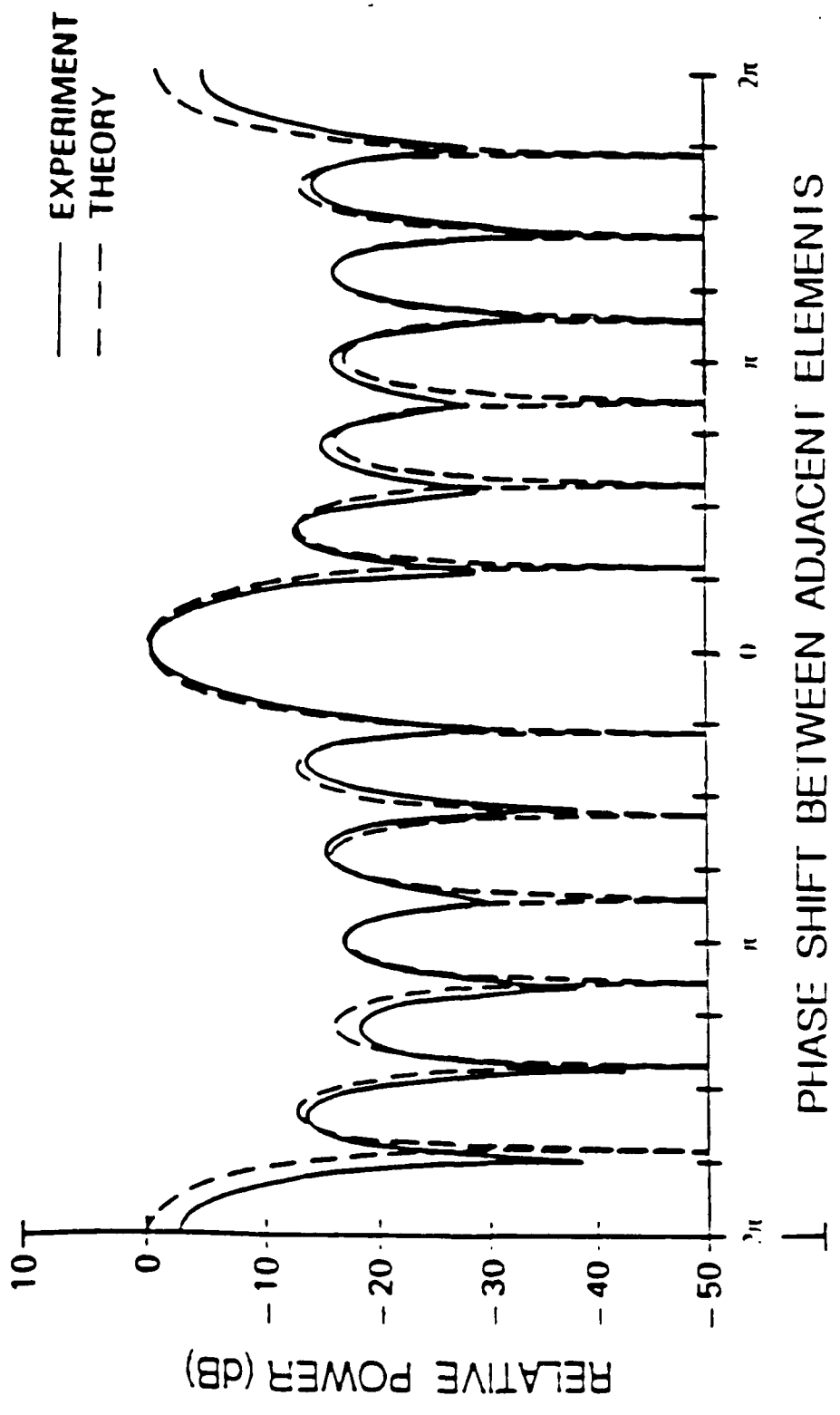

Fig. III-6 — Seven element array factor pattern

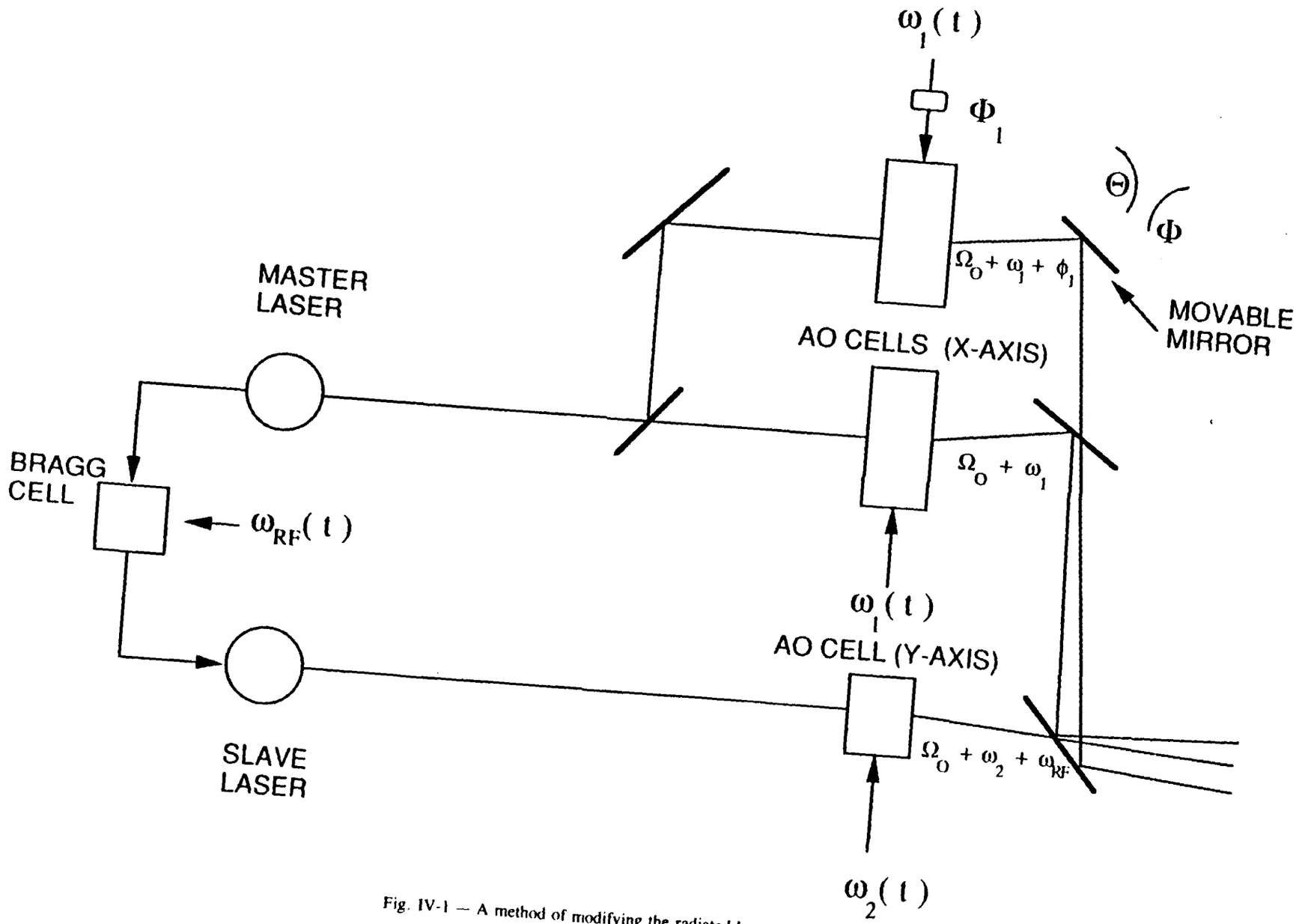

Fig. IV-1 — A method of modifying the radiated beam pattern, e.g., for creating a null

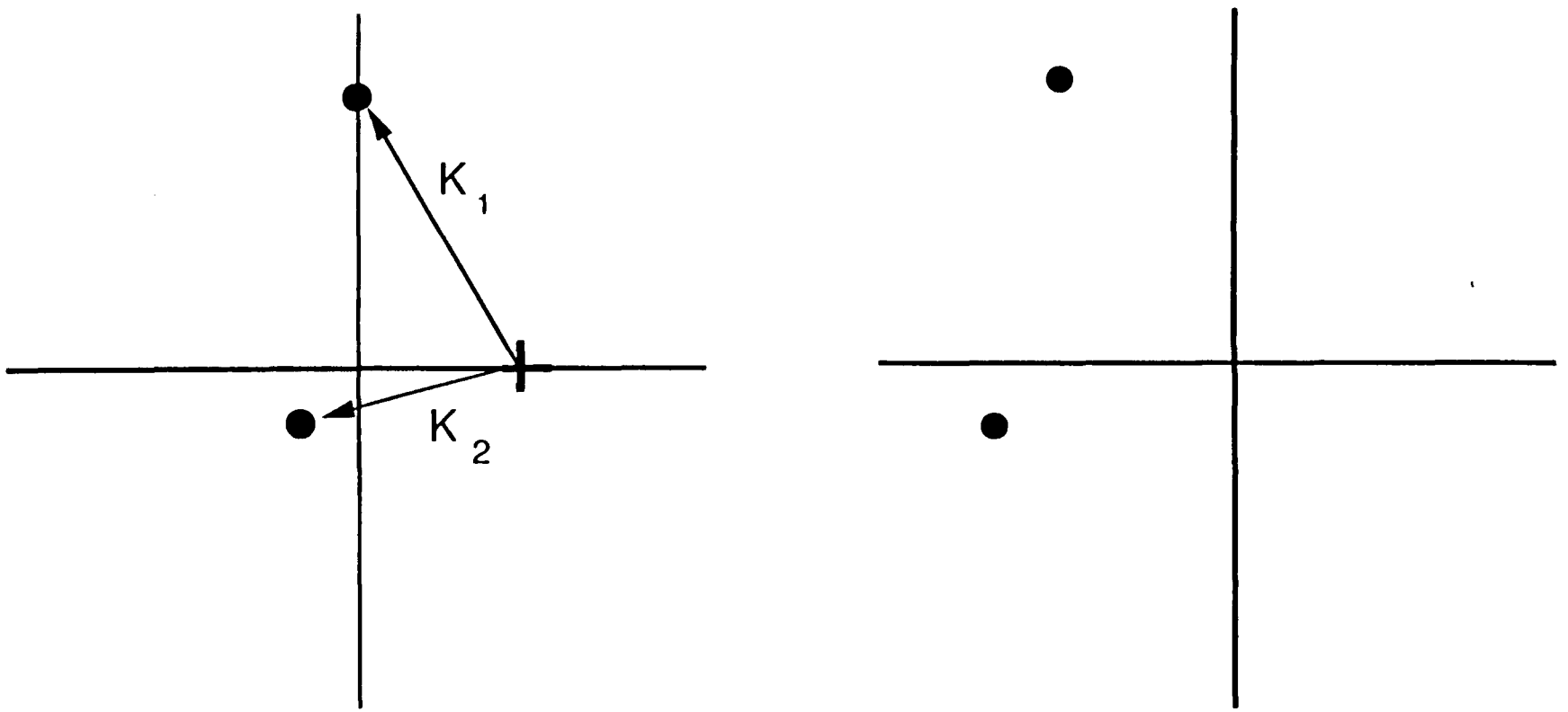

Fig. IV-2 — K/Beam Space diagram for a parasitic beam

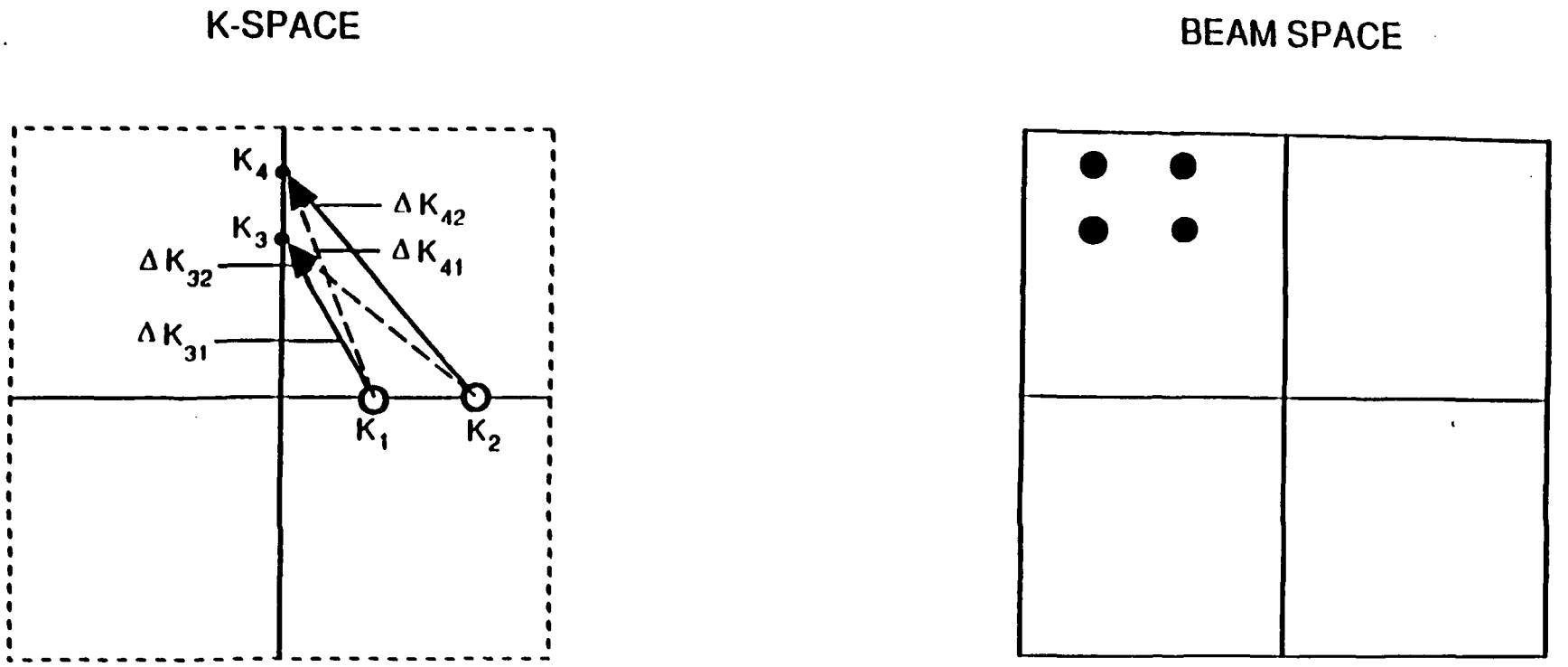

CHANNEL 1: $\omega_{RF} + \Delta\omega_Y - \Delta\omega_X + \delta\omega_Y - \delta\omega_X$

CHANNEL 2: $\omega_{RF} + \Delta\omega_Y - \Delta\omega_X + \delta\omega_Y$

CHANNEL 3: $\omega_{RF} + \Delta\omega_Y - \Delta\omega_X - \delta\omega_X$

CHANNEL 4: $\omega_{RF} + \Delta\omega_Y - \Delta\omega_X$

Fig. IV-3 — Monopulse beamforming by the injection of two control frequencies into each AOBD

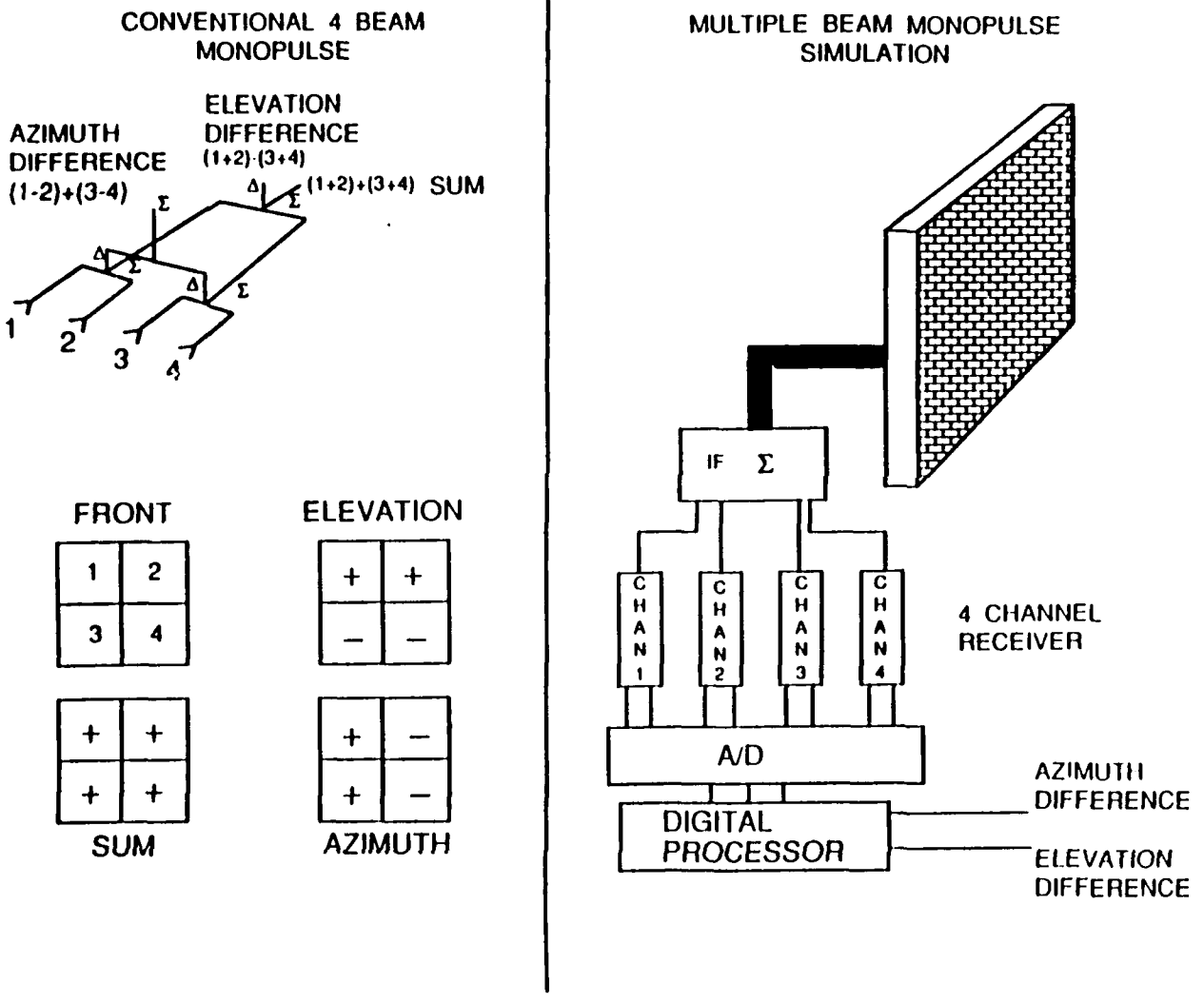

Fig. IV-4 — Comparison of conventional and optical monopulse concepts

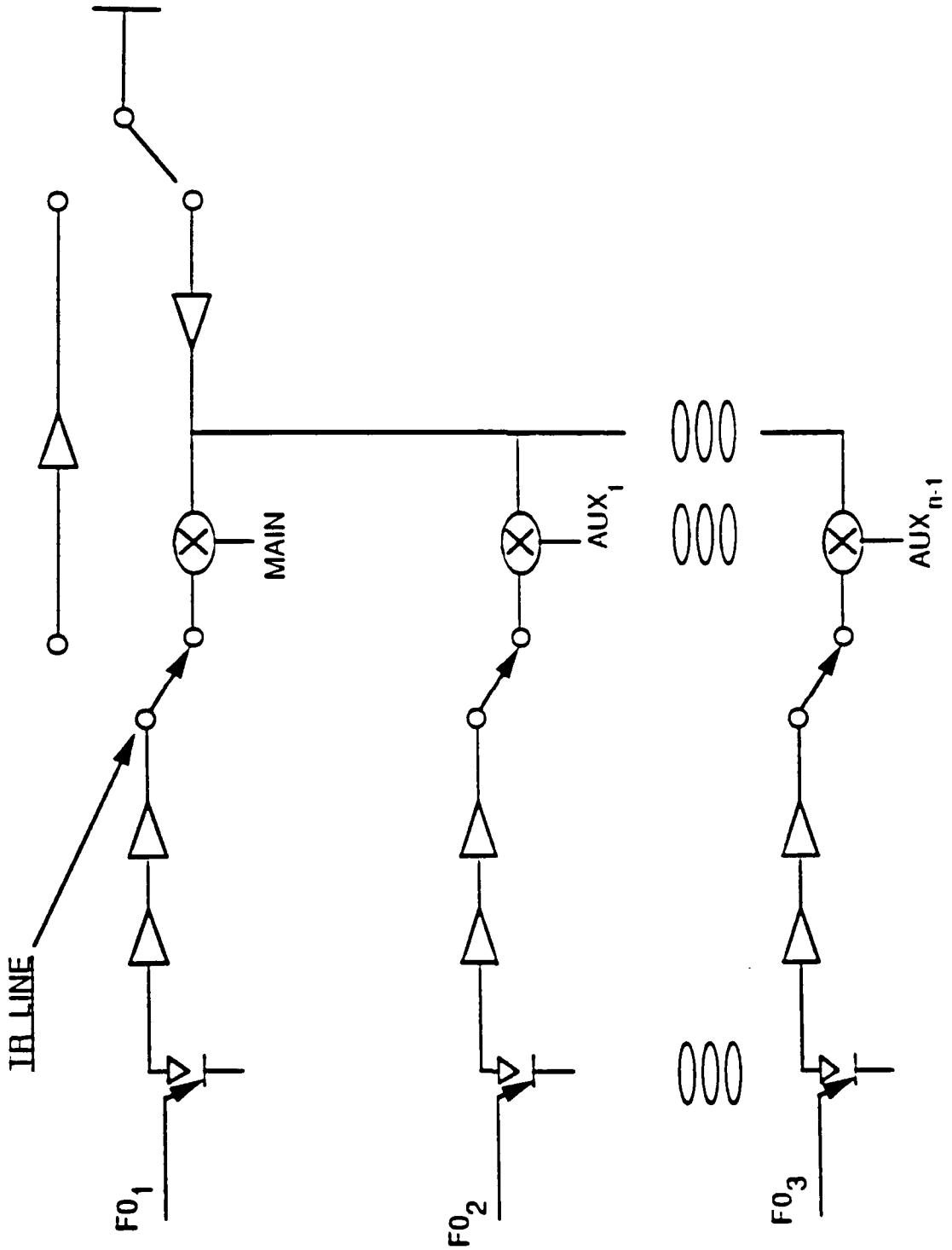

Fig. IV-5 — Multiple receive beams using parallelism in the TR module

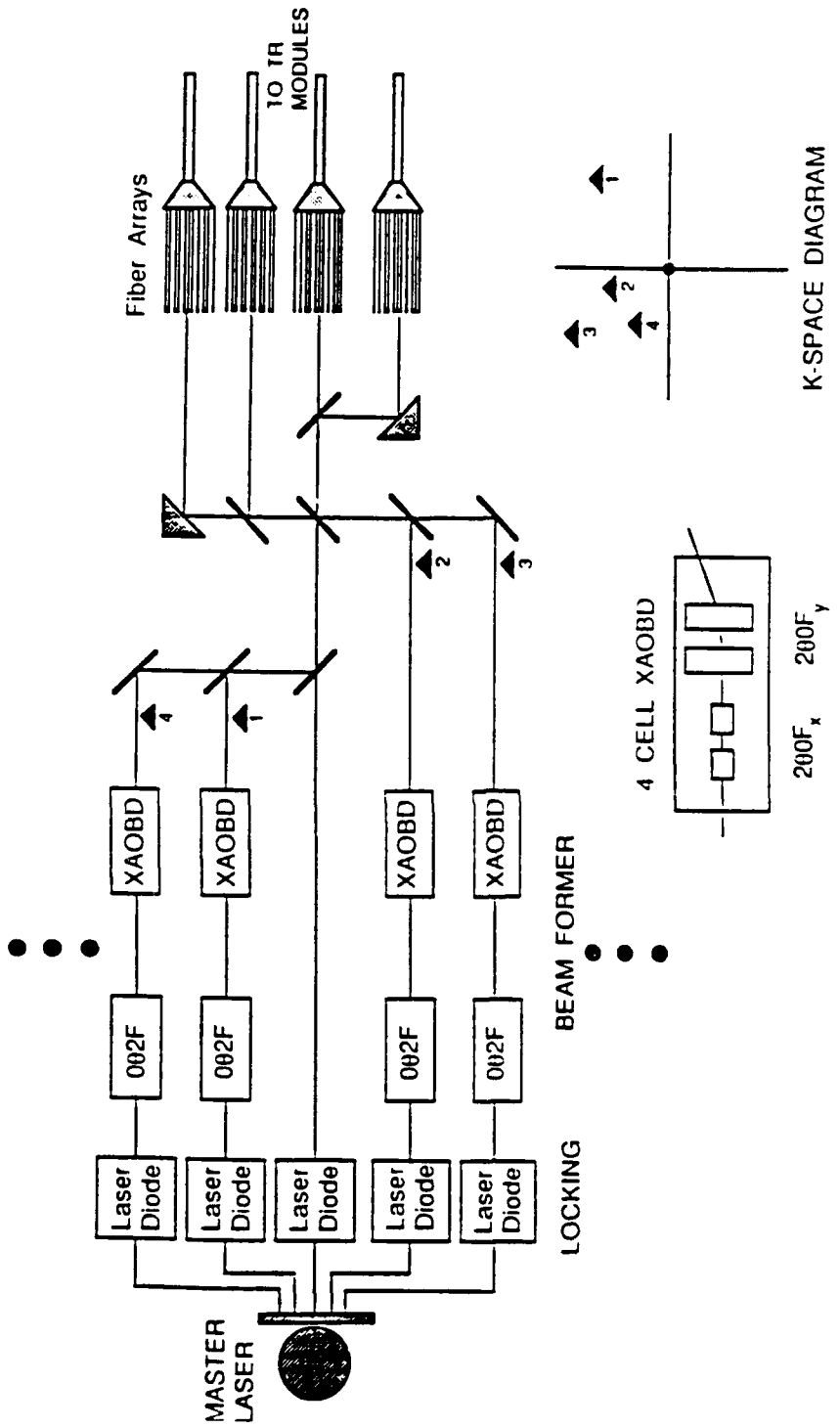

Fig. IV-6 — Multiple receive/transmit beams using optical parallelism

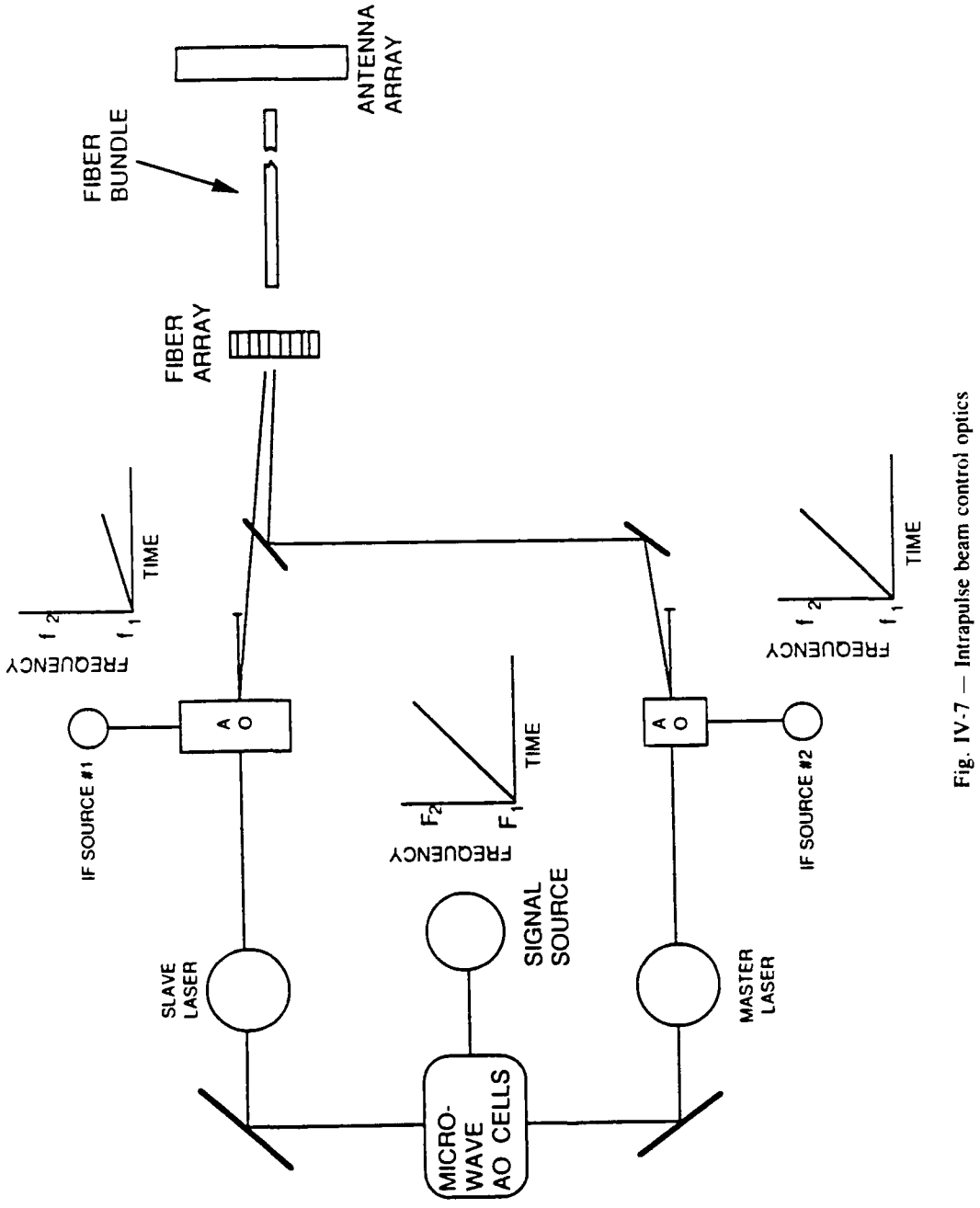

Fig. IV-7 — Intrapulse beam control optics

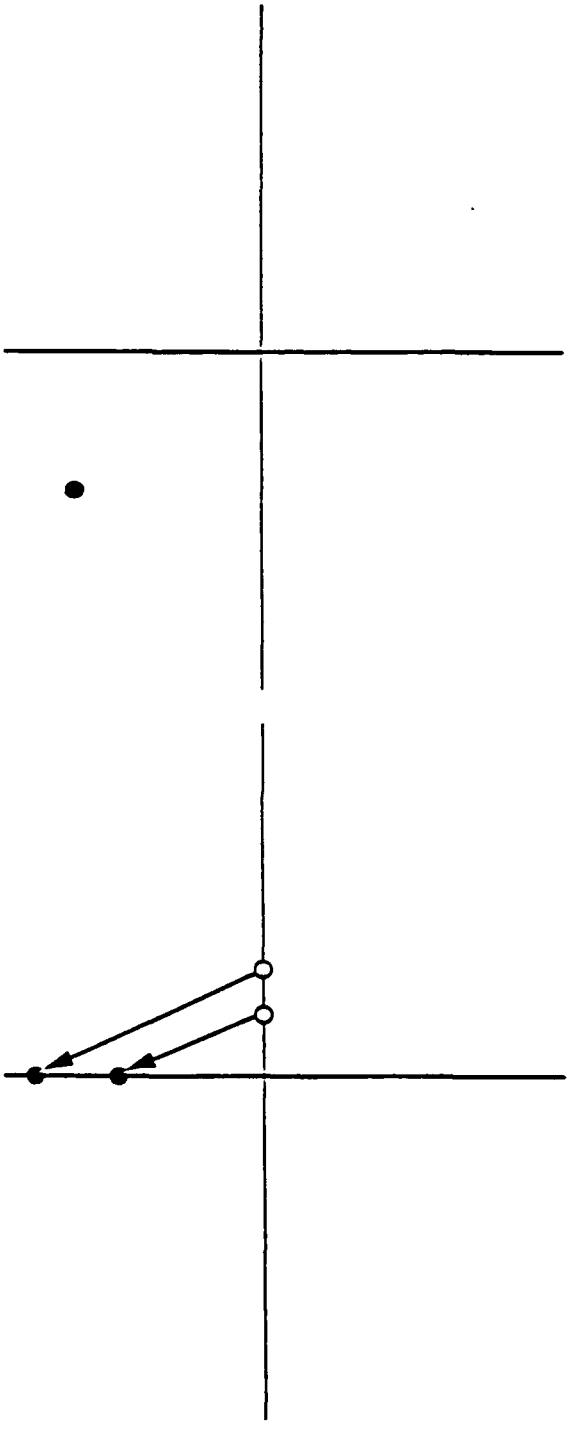

Fig. IV-8 — K/Beam Space diagram for intrapulse steered chirp waveform

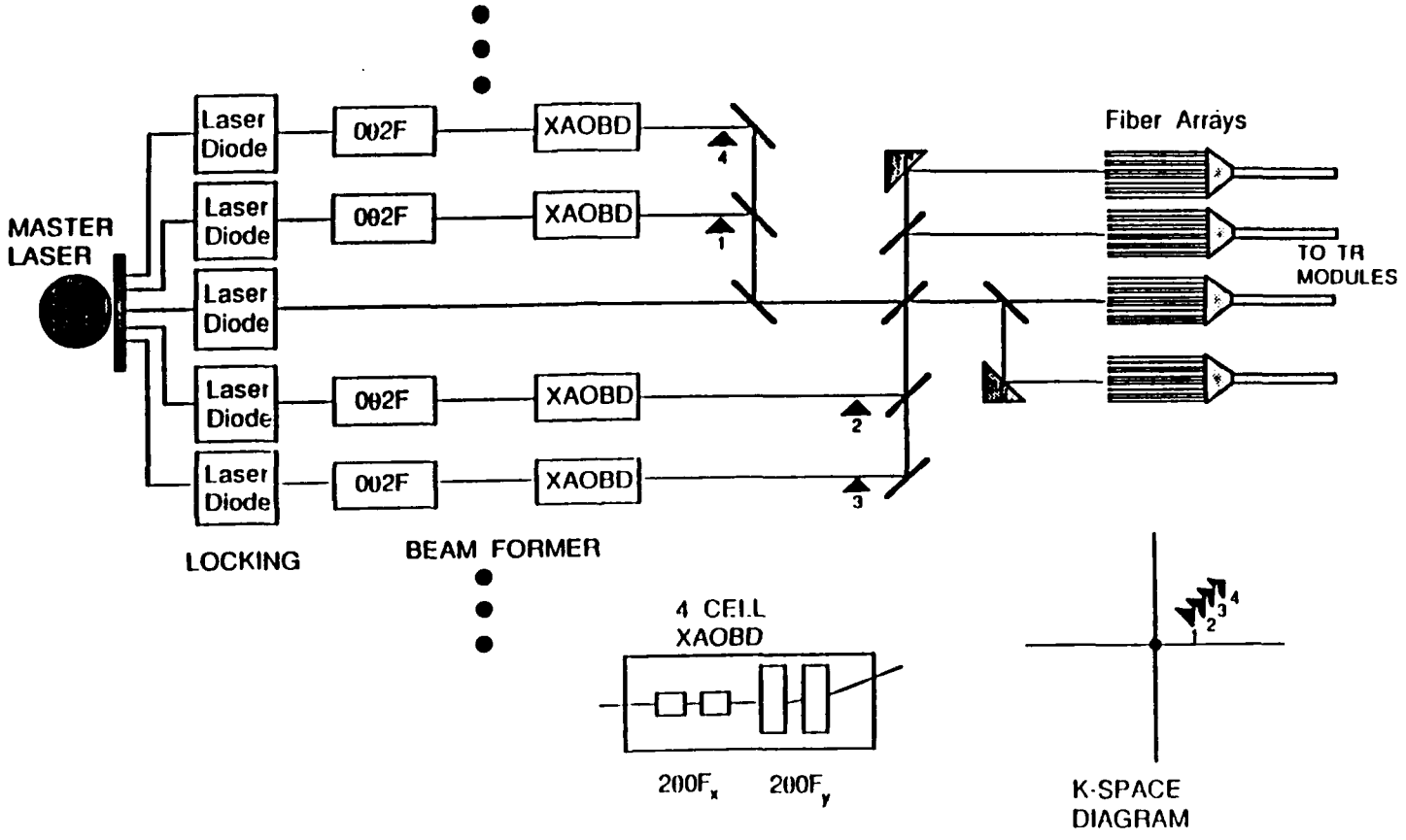

Fig. IV-9 — Multiple contiguous subband beamforming for wideband operation

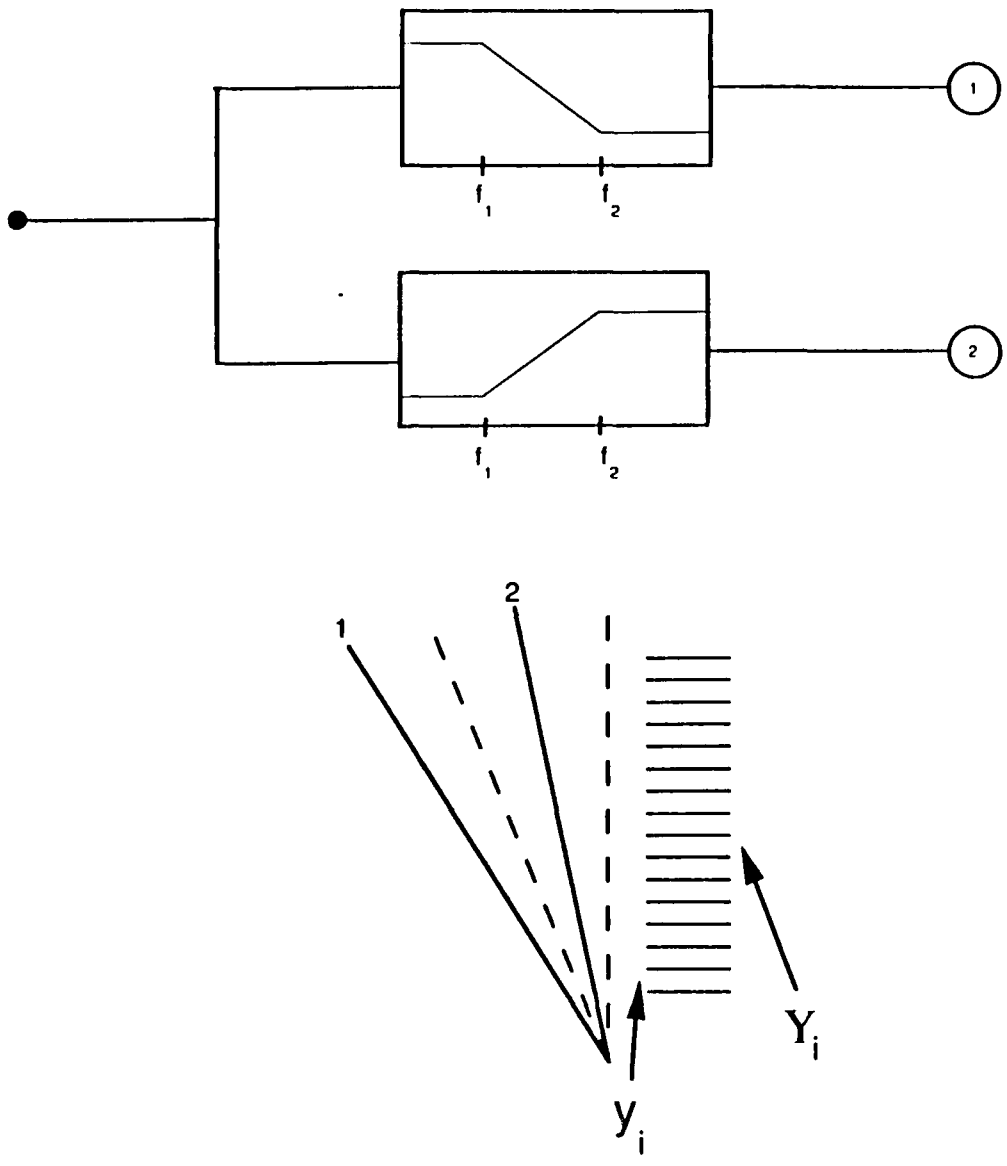

Fig. IV-10 — Two beamport drive circuit for wideband beamforming

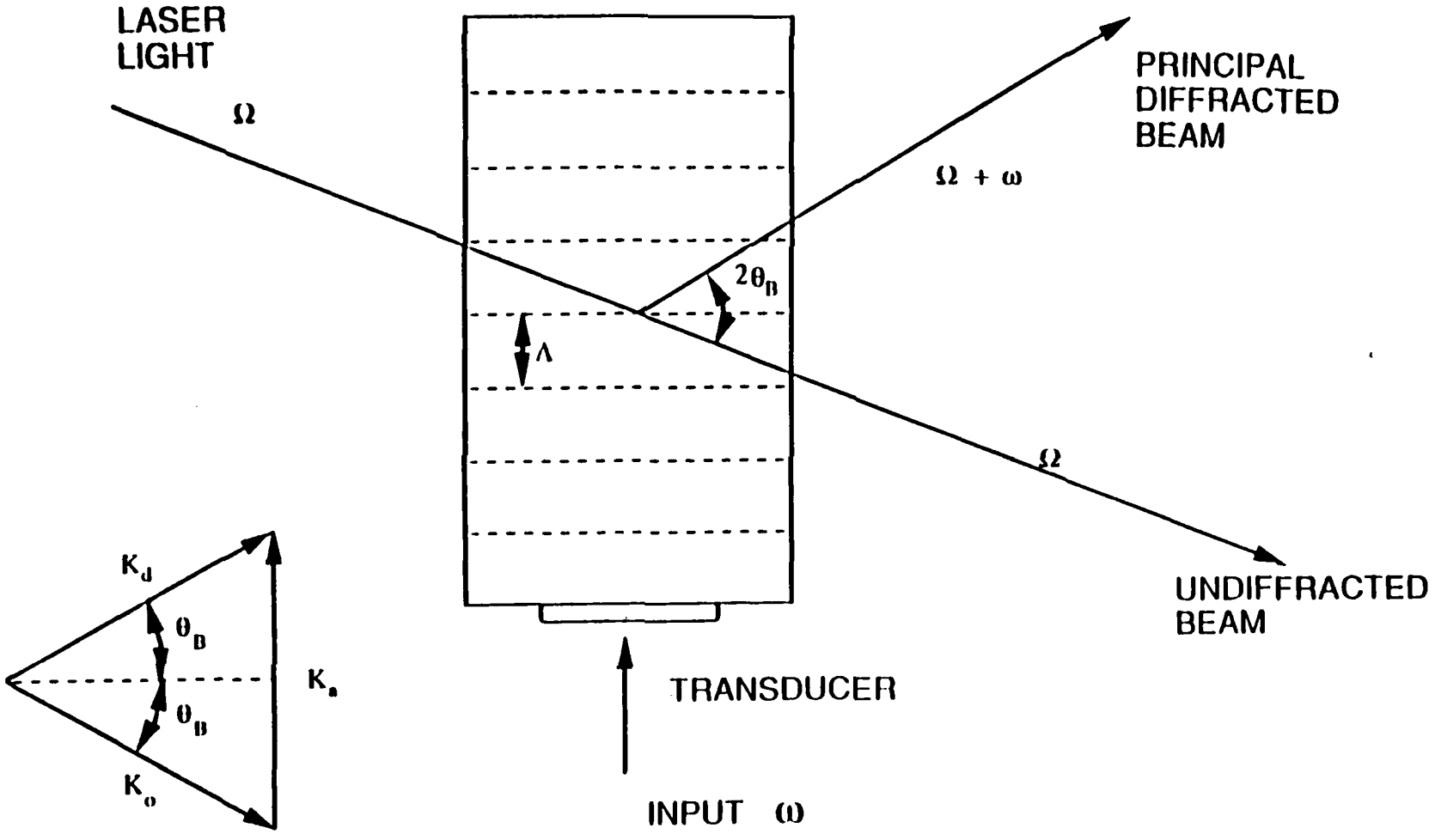

Fig. V-1 — Bragg cell interaction diagram

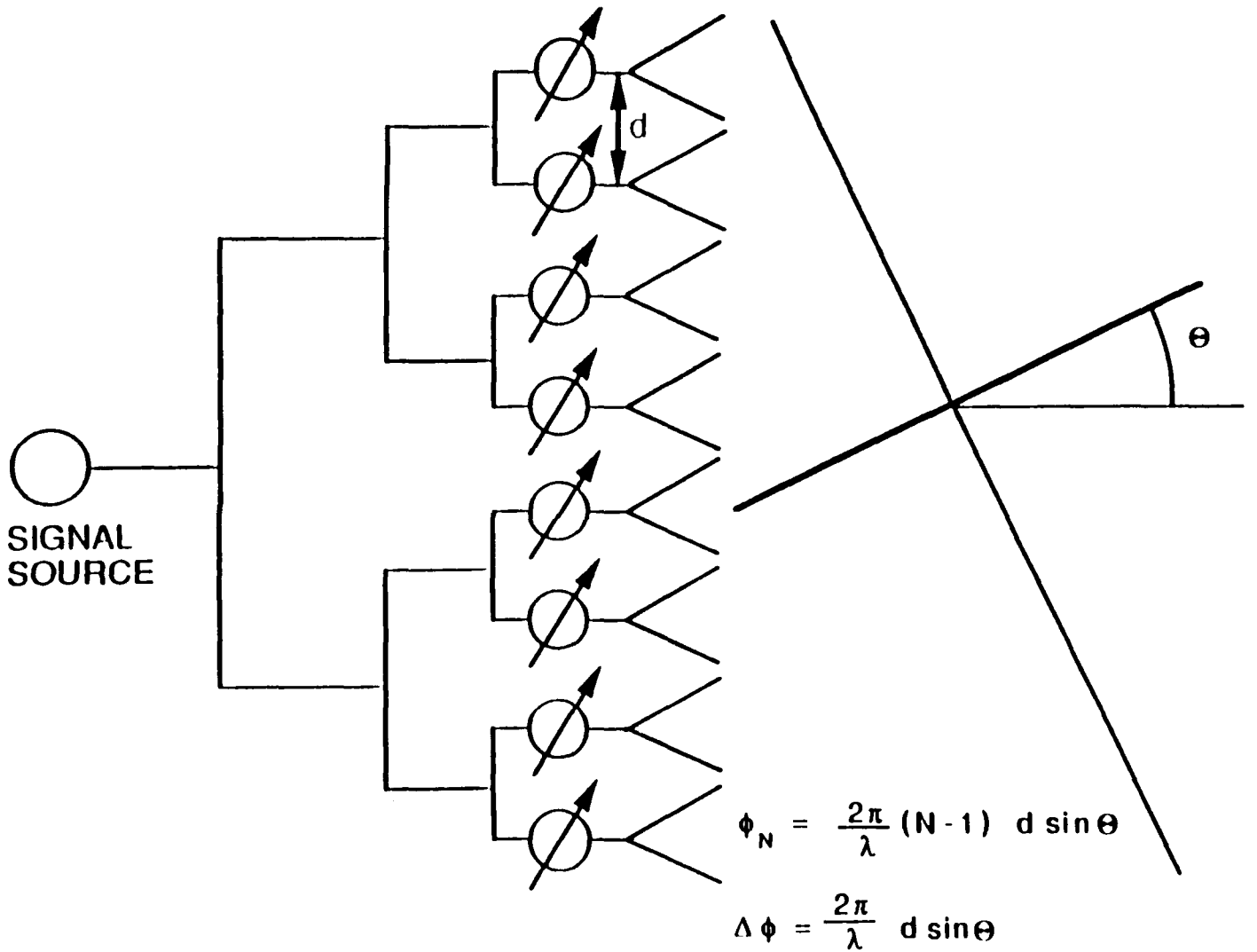

Fig VI-2 — Conventional, corporate fed, phase steered array beamformer